bioRxiv preprint doi: https://doi.org/10.64898/2026.03.30.715073; this version posted April 1, 2026. The copyright holder for this preprint (which was not certified by peer review) is the author/funder, who has granted bioRxiv a license to display the preprint in perpetuity. It is made available under a CC-BY 4.0 International license.

Identification of *SNARE* Genes in Cucumber and the Role of *CsSYP121* in Salt Stress Response

Weijuan Zhou[1,2,3,#], Jie Zheng[1,#], Shengjun Zhou[1], Yue Guo[1,2,3], Dongmei Kong[1], Pu Yang[1], Ben Zhang[1,2,3*]

[1]School of Life Science, Shanxi University, Taiyuan, Shanxi, 030006, China

[2]Shanxi Key Laboratory for Research and Development of Regional Plants, Shanxi University, Taiyuan, Shanxi, 030006, China

[3]Key Laboratory of Chemical Biology and Molecular Engineering of Ministry of Education, Taiyuan, Shanxi, 030006, China

#Weijuan Zhou and Jie Zheng contributed equally to this work.

*Corresponding Authors: Ben Zhang ORCID:0000-0003-4473-9184 Email: benzhang@sxu.edu.cn

Abstract

Soluble N-ethylmaleimide-sensitive factor attachment protein receptors (SNAREs) are essential regulators of plant growth, development, and stress adaptation. In this study, we performed a comprehensive genome-wide identification of *SNARE* genes in cucumber (*Cucumis sativus* L.), uncovering 51 putative members designated as *CsSNAREs*. Phylogenetic analysis confirmed that these genes cluster into five major clades: *Qa-CsSNARE* (14), *Qb-CsSNARE* (9), *Qc-CsSNARE* (10), *Qb+c-CsSNARE* (3), and *R-CsSNARE* (15). Bioinformatic analysis of their promoter regions, coupled with expression profiling under diverse abiotic stress conditions, highlighted a heightened responsiveness within the *Qa-CsSNARE* subfamily. To validate this, we selected representative *Qa-CsSNARE* genes for quantitative real-time PCR analysis under drought and salt stress. Among these, *CsSYP121* was notably induced by salt treatment. We subsequently generated transgenic cucumber lines overexpressing *CsSYP121* and challenged them with salinity. Phenotypic assessment, combined with measurements of reactive oxygen species (ROS) accumulation and K^+/Na^+ ratios, demonstrated that *CsSYP121* overexpression (OE) confers enhanced salt tolerance and boosts antioxidant capacity. We propose a model wherein *CsSYP121* mitigates ROS-induced cellular damage under salt stress, potentially through promoting K^+/Na^+ homeostasis, thereby improving plant performance under saline conditions. Our findings identify *CsSYP121* as a promising candidate gene for breeding salt-tolerant crops.

bioRxiv preprint doi: https://doi.org/10.64898/2026.03.30.715073; this version posted April 1, 2026. The copyright holder for this preprint (which was not certified by peer review) is the author/funder, who has granted bioRxiv a license to display the preprint in perpetuity. It is made available under a CC-BY 4.0 International license.

Keywords:

Cucumber, SNARE, *CsSYP121*, salt stress, ROS, K^+/Na^+ homeostasis

1. Introdution

Interorganellar communication in plant cells relies critically on membrane integrity and functional dynamics. This communication regulates cellular homeostasis, coordinated growth, and developmental transitions (Gu et al., 2020; Kwon et al., 2020; Zhang et al., 2020). The soluble N-ethylmaleimide-sensitive factor attachment protein receptor (SNARE) protein family are known to be involved in vesicle trafficking through driving membrane fusion (Hong, 2005). SNARE proteins typically range in size from 100 to 300 amino acids and often contain at least one region approximately 60 amino acid residues long, called SNARE motif. These proteins interact with each other to form SNARE complexes, which mediate vesicular fusion. Based on their subcellular localization, SNARE proteins can be classified into t (target)-SNAREs and v (vesicle)-SNAREs. In addition, SNARE members exhibit distinct classification based on amino acid residues within their central layer, leading to the designation of Q (glutamine-rich) and R (arginine-rich) sub-families (Fasshauer et al., 1998). The Q subgroup includes Qa-, Qb-, Qc-, and Qb+c-SNAREs. Structurally, most Q-SNAREs have an N-terminal autoinhibitory Habc domain (triple helical motifs Ha, Hb, Hc), a core SNARE motif, and a C-terminal transmembrane domain (Zhang et al., 2020). Vesicle fusion typically requires three Q-SNAREs and one R-SNARE (Cermesoni et al., 2024; Zhang et al., 2020).

SNARE proteins function in key plant processes, including phytohormone signaling (Xia et al., 2020; Xue et al., 2018), pathogen defense (Waghmare et al. 2018; Zhu et al. 2024), stress adaptation (Kwon et al., 2020; Nisa et al., 2017; Waghmare et al., 2024), gravity perception (Yano et al., 2003), cell plate assembly (Zhang et al., 2011), and arbuscular mycelium morphogenesis (Huisman et al., 2016; Sogawa et al., 2019).

SNARE genes are identified in many plants, including Arabidopsis, wheat (*Triticum aestivum*), rice (*Oryza sativa*), Chinese cabbage (*Brassica rapa*), grapevine (*Vitis vinifera*), *Brassica napus*, and foxtail millet (*Setaria italica*) (Bassham et al., 2008; Zhang et al., 2018; G. Wang et al., 2021; Xu et al., 2022; H. Wang et al., 2021; Zeng et al., 2024). Plants possess more *SNARE* genes than animals or

bioRxiv preprint doi: https://doi.org/10.64898/2026.03.30.715073; this version posted April 1, 2026. The copyright holder for this preprint (which was not certified by peer review) is the author/funder, who has granted bioRxiv a license to display the preprint in perpetuity. It is made available under a CC-BY 4.0 International license.

61 microorganisms, suggesting roles in complex plant physiology. In *Marchantia polymorpha*, some
62 SNARE localizations differ from Arabidopsis homologs; for example, Qa-SNAREs MpSYP12A and
63 MpSYP12B localize to oil bodies involved in lipid metabolism (Kanazawa et al., 2016). Some Qa- and
64 R-SNAREs also regulate membrane transporters or ion channels via direct interactions, affecting ion
65 homeostasis. This is crucial for plant growth and abiotic stress responses, especially to drought and
66 salinity (Grefen et al., 2015; Xia et al., 2019; Zhang et al., 2022, 2020, 2015).

67 Qa-SNARE SYP121 and SYP122 are conserved in vegetative plants (Sanderfoot 2007; Waghmare
68 et al. 2018). They share high sequence similarity and form a SNARE complex with Qb+c-SNARE
69 SNAP33 and R-SNAREs VAMP721. This complex mediates vesicle trafficking to the plasma
70 membrane, linked to biotic stress responses (Karnik et al. 2013; Waghmare et al. 2018; Enami et al.
71 2009; Kwon et al. 2020, 2008). In Arabidopsis, single *syp121* or *syp122* mutations show minimal
72 effects, but double mutations are lethal, indicating functional redundancy (Karnik et al., 2017).
73 However, SYP121 and SYP122 mediate distinct secretory pathways (Waghmare et al. 2018). Recent
74 research reveals that SYP121 physically interacts with potassium channels KAT1 and KC1, regulating
75 their gating and linking vesicle trafficking to potassium homeostasis (Grefen et al., 2010a, 2015).
76 SEC11, a Sec1/Munc18 protein, selectively interacts with SYP121 via $R^{20}R^{21}$ residues to regulate
77 SNARE-channel complex formation (Zhang et al., 2019). These findings highlight SYP121's critical
78 role in plant growth and development.

79 Cucumber, *Cucumis sativus* L., is a nutrient-dense, low-calorie vegetable rich in vitamin C, fiber,
80 and water, is globally significant (Huang et al., 2009). Cucumber is one of the most water-loving
81 vegetable crop, it is sensitive to salt and drought stress (Das et al., 2024; Li et al., 2023; Wang et al.,
82 2018). However, studies on cucumber *SNARE* genes are limited. The recent near-complete cucumber
83 genome (Guan et al., 2024), enabling systematic investigations into cucumber genes, particularly the
84 *CsSNARE* genes.

85 In this research, we conducted a systematic screening and successful identification of the
86 *CsSNARE* gene family within the cucumber genome. Furthermore, the expression profiles of key
87 *Qa-CsSNARE* genes were rigorously characterized following exposure to both drought and salt stresses,
88 thereby establishing a foundational understanding necessary for elucidating their potential
89 contributions to abiotic stress tolerance mechanisms. To probe the role of individual members, we
90 developed *CsSYP121*-overexpressing cucumber lines and evaluated their performance, including

bioRxiv preprint doi: https://doi.org/10.64898/2026.03.30.715073; this version posted April 1, 2026. The copyright holder for this preprint (which was not certified by peer review) is the author/funder, who has granted bioRxiv a license to display the preprint in perpetuity. It is made available under a CC-BY 4.0 International license.

growth, development, and physiological responses under salt stress. These results offer valuable molecular insights for future functional studies aimed at enhancing crop resilience and provide new genetic resources for improving salt tolerance in cucumber breeding programs.

2. Materials and methods

2.1 Identification of the CsSNARE gene family

The Cucumber (Chinese Long) v4 genome dataset was obtained from the Cucumber Genome Database (http://www.cucumberdb.com, accessed on 05 May 2025) (Guan et al., 2024). Candidate *CsSNARE* genes identified through BLAST analysis of Arabidopsis SNARE sequences (retrieved from The Arabidopsis Information Resource, https://www.arabidopsis.org, accessed on 05 May 2025) in the cucumber genome. The truncated open reading frames, peptides <100 amino acids, and redundant sequences were removed. For the validated CsSNARE proteins, theoretical isoelectric points (pI), molecular weights (MW), and amino acid compositions were predicted using ExPASY (http://web.expasy.org/protparam, accessed on 03 June, 2025) (Gasteiger, 2003) .

2.2 Phylogenetic analysis and chromosomal localization of the cucumber CsSNARE gene family

For phylogenetic analysis, full-length SNARE protein sequences from *Arabidopsis thaliana*, *Oryza sativa* and *Cucumis sativus* were aligned using MEGA X v10.2 (https://www.megasoftware.net, accessed on 02 June, 2025) (Kumar et al., 2018). Multiple sequence alignment was performed prior to constructing a maximum-likelihood (ML) phylogenetic tree with 1,000 bootstrap replicates. The resulting tree was refined and visualized using iTOL v7 (https://itol.embl.de/, accessed on 02 June, 2025). A combined phylogenetic tree was generated for systematic classification of *CsSNARE* genes, with gene nomenclature assigned according to evolutionary relationships. Functional annotations for identified *CsSNARE* genes were extracted from the genome reference GFF3 file. Chromosomal coordinates of *CsSNARE* sequences were mapped using TBtools v2.154 (https://github.com/CJ-Chen/TBtools/releases, accessed on 02 June, 2025) (Chen et al., 2023) to generate a physical location map.

bioRxiv preprint doi: https://doi.org/10.64898/2026.03.30.715073; this version posted April 1, 2026. The copyright holder for this preprint (which was not certified by peer review) is the author/funder, who has granted bioRxiv a license to display the preprint in perpetuity. It is made available under a CC-BY 4.0 International license.

2.3 Conserved motifs, promoter analyses, and gene structure analysis of CsSNARE

Conserved motifs of CsSNARE proteins were identified using the Multiple Expectation Maximization for Motif Elicitation (MEME) suite (https://meme-suite.org/meme/, accessed on 03 June, 2025). Gene structures comprising intron-exon organization were characterized via the Gene Structure Display Server (http://gsds.cbi.pku.edu.cn/, accessed on 03 June, 2025) (Hu et al., 2015). For promoter analysis, 2,000 bp upstream sequences flanking cucumber *CsSNARE* genes were submitted to PlantCARE (https://bioinformatics.psb.ugent.be/webtools/plantcare, accessed on 03 June, 2025) (Lescot et al., 2002) to investigate cis-acting elements.

2.4 Duplication and covariance analysis of CsSNARE genes

CsSNARE gene duplication events were analyzed using the MCScanX of TBtools, with the criterion of long genes covering 75% of the comparable sequence and 75% of the similarity comparison region in length. Covariance analysis was performed using TBtools among cucumber, *Oryza sativa*, and Arabidopsis, respectively.

2.5 In silico expression profiling of CsSNARE genes

To investigate the tissue-specific and developmental expression profiles of *CsSNARE* genes in cucumber, as well as their responsiveness to diverse abiotic (cold, heat, salt) and biotic stresses (Angular leaf spot, Gray mold, Powdery mildew, *Cladosporium cucumerinum*), we retrieved relevant expression datasets from the Cucumber-DB database (http://www.cucumberdb.com/, accessed on 07 June, 2025). Subsequent expression profiling analysis was performed using TBtools software.

2.6 Plant materials, growth conditions, and treatments

Cucumber seeds (commercial cultivar 9930) were acquired from Weimibio Co., Ltd. and utilized exclusively for research purposes. The *CsSYP121* gene (*CsaV4_6G002929*) was amplified from

bioRxiv preprint doi: https://doi.org/10.64898/2026.03.30.715073; this version posted April 1, 2026. The copyright holder for this preprint (which was not certified by peer review) is the author/funder, who has granted bioRxiv a license to display the preprint in perpetuity. It is made available under a CC-BY 4.0 International license.

cucumber leaf tissue and subsequently cloned into a plant transformation vector (driven by the CaMV 35S promoter, vector acquired from Weimibio Co., Ltd.). The result construct was verified by Sanger sequencing (Sangon Biotech). The recombinant plasmid was introduced into *A. tumefaciens* strain EHA105 via freeze-thaw transformation. Agrobacterium-mediated cucumber transformation was performed by Weimibio Co., Ltd. (http://www.wimibio.com), following established protocols. Briefly, cotyledon explants from 2-day-old germinated cucumber line 9930 seedlings were incubated with 50 mL of recombinant *A. tumefaciens* (OD_{600}=0.6) suspension for 30 minutes at 28°C. Following this, explants underwent sequential co-culture phases: an initial 3-day dark incubation at 23 °C followed by 7 days under illumination at 25 °C. The light source was cool white fluorescent tubes (Philips TL-D 36W/33-640, color temperature 4,100 K, spectrum 400–700 nm), providing a photosynthetic photon flux density (PPFD) of approximately 71 $\mu mol \cdot m^{-2} \cdot s^{-1}$, with a photoperiod of 16 h light/8 h dark. Infected tissues were then washed and transferred to shoot induction medium (SIM) supplemented with 50 mg/L spectinomycin, with explants subcultured onto fresh SIM every two weeks during the six-week selection period. Adventitious shoot meristems typically emerged from the cut edges of cotyledon explants after 2–3 weeks of culture on SIM. Surviving explants were subsequently transferred to elongation and rooting media containing the same antibiotic concentration. All tissue culture procedures were performed under strictly sterile conditions in laminar flow hoods, with cultures maintained in sterile vessels (Magenta boxes or parafilm-sealed Petri dishes); non-sterile greenhouse conditions were introduced only after regenerated plantlets with well-developed root systems were successfully acclimatized. Putative transgenic lines, confirmed by PCR analysis using *aadA* gene-specific flanking primers, were acclimatized in greenhouse conditions for seed production.

The *CsSYP121* over-expressing (OE) seeds were germinated in a tray containing vermiculite and nutrient soil at a ratio of 1:1 and cultivated in the growth chamber under the following conditions: temperature of 25-30℃, a light intensity of 250 $\mu mol \cdot m^{-2} \cdot s^{-1}$, a photoperiod of 16 h (day)/8 h (night), and a relative humidity of 40-50%. When the cucumber seedlings reached three leaves and one heart stage (three fully expanded cotyledons and visible apical meristem), the plants with consistent growth condition were selected for drought stress. Plants were randomly allocated to two treatment groups: (1) well-watered control; (2) drought-stressed treatment subjected to complete water withholding for 14 days; (3) salt-stressed treatment subjected to 150 mmol/L NaCl for 10 days

bioRxiv preprint doi: https://doi.org/10.64898/2026.03.30.715073; this version posted April 1, 2026. The copyright holder for this preprint (which was not certified by peer review) is the author/funder, who has granted bioRxiv a license to display the preprint in perpetuity. It is made available under a CC-BY 4.0 International license.

(Zhou et al., 2022). Each treatment comprised three biological replicates with ten plants per replicate. Leaf tissue samples were collected at predetermined time points from the second fully expanded leaf. Harvested samples were immediately frozen in liquid nitrogen and stored at -80°C prior to downstream analysis.

2.7 RNA extraction and qRT-PCR

The RNA extraction and qRT-PCR were performed as described before (Fan et al., 2024; Guo et al., 2024; Liang et al., 2024). Total RNA was extracted using TransZol™UP Plus RNA Kit (TransGen Biotech, Beijing, China). The first-strand cDNA was synthesized using EasyScript® One-Step gDNA Removal and cDNA Synthesis SuperMix Kit (TransGen Biotech, Beijing, China) according to the manufacturer's instructions. The primers of *CsSNARE* genes were synthesized by Shanghai Sangon Biotech (As shown in supplement Table 1). *CsEF1α* (*CsaV4_5G001996*) and *CsCACS* (*CsaV4_3G004932*) were used as internal references. Quantitative real-time PCR (qRT-PCR) was performed using PerfectStart® Green qPCR SuperMix Kit (TransGen Biotech, Beijing, China). Each experiment included three technical replicates and three biological replicates to ensure the reliability of the results.

2.8 Western blot

To verify protein expression, plant tissue extracts were subjected to immunoblot (Western blot) analysis using an anti-CsSYP121 antibody, as previously described (Zhang et al., 2018).

2.9 Analysis of cation contents, H_2O_2 accumulation, and antioxidant enzyme activities

The leaf samples were collected as described above. The analysis of cation content was conducted by Qidian Chemical Technology Service (Liaocheng, China) as previous described (Chen et al., 2016; Grefen et al., 2015; Guo et al., 2024; Liu et al., 2023). After harvesting, the samples underwent acid digestion. The concentrations of Na^+ and K^+ ions were determined using inductively coupled plasma optical emission spectrometry (ICP-OES 730, Agilent, USA).

The determination of indicators related to ROS was conducted using commercial kits from

bioRxiv preprint doi: https://doi.org/10.64898/2026.03.30.715073; this version posted April 1, 2026. The copyright holder for this preprint (which was not certified by peer review) is the author/funder, who has granted bioRxiv a license to display the preprint in perpetuity. It is made available under a CC-BY 4.0 International license.

Suzhou Keming Biotechnology Co. ltd (China), aligning with prior research (Guo et al., 2024). Fresh leaf tissue (0.1 g) was homogenized in 1 mL of the specific extraction buffer provided with each kit on ice, followed by centrifugation at 12,000 × g for 15 min at 4°C. The resulting supernatant was used for subsequent assays. Specifically, the contents of hydrogen peroxide (H_2O_2, H_2O_2-2-Y), along with the activities of catalase (CAT, CAT-2-Y), superoxide dismutase (SOD, SOD-2-Y), and peroxidase (POD, POD-2-Y) were assessed. Peroxidase (POD) Activity was determined using the POD-2-Y kit. The assay measures the oxidation of guaiacol in the presence of H_2O_2. The reaction mixture contained 50 mM phosphate buffer (pH 7.0), 20 mM guaiacol, 10 mM H_2O_2, and enzyme extract. The increase in absorbance at 470 nm due to tetraguaiacol formation (ε_{470}= 26.6 $mM^{-1}cm^{-1}$) was recorded. One unit of POD activity was defined as an absorbance change of 0.01 per minute per mg protein. This method primarily detects the activity of class III (guaiacol-type) peroxidases.

2.10 Detection of protein subcellular localization

The template cDNA for the cloning of CsSYP121 was derived from the aforementioned reverse transcription. Amplification primers were designed to span the coding sequence (CDS) region of the target gene, excluding the promoter sequence, with the objective of obtaining the open reading frame (ORF) for subsequent Agrobacterium tumefaciens-mediated transient expression assays in tobacco. High-fidelity DNA polymerase KOD FX was employed to ensure amplification accuracy, and all primers were synthesized by Shanghai Sangon Biotechnology Co., Ltd. (detailed in Supplementary Table 1). Gateway® attB1 and attB2 recombination sites were incorporated into the amplicons. Entry clones were constructed via BP recombination using the pDONR207 vector (Invitrogen), and the final expression clones were generated through LR recombination utilizing LR Clonase™ II enzyme mix (Invitrogen).

To investigate the protein localization, *CsSYP121* was cloned into the pUBN-GFP-DEST vector via LR reaction, following established protocols (Grefen et al., 2010b; Zhang et al., 2015). And AtAHA1 was cloned into the pUBC-YFP-DEST vector as a marker via the same LR reaction. *Agrobacterium tumefaciens* GV3101 harboring this construct was used to infiltrate tobacco (*Nicotiana tabacum*) leaves, as previously described (Zhang et al., 2015). GFP fluorescence was

bioRxiv preprint doi: https://doi.org/10.64898/2026.03.30.715073; this version posted April 1, 2026. The copyright holder for this preprint (which was not certified by peer review) is the author/funder, who has granted bioRxiv a license to display the preprint in perpetuity. It is made available under a CC-BY 4.0 International license.

observed and imaged using a confocal laser scanning microscope at 48-72 h post-transfection. For the GFP localization analysis, confocal microscopy was performed using a Leica STELLARIS 5 equipped with a 20× objective. The GFP signal was excited with a 488 nm laser and detected through a 505-530 nm bandpass filter.

2.11 Statistical analysis

The sample size (n) for each comparison refers to the number of biological replicates. Statistical analysis of independent experiments was reported as means±SE as appropriate, with signifcance determined by Student's t-test or ANOVA.

3. Results

3.1 Identification of CsSNARE genes in cucumber

Based on the sequence of homology with Arabidopsis, we identified 94 putative *CsSNARE* gene candidates in cucumber. Through analysis of protein length and structural integrity, 51 members of the *CsSNARE* gene family were finally obtained and named according to their affinities to homologous of Arabidopsis and *O. sativa* (Table 1). Bioinformatic analysis revealed substantial diversity in molecular mass (10.9-37.5 kDa) across the CsSNARE family, except for the Tomosyn-like R-CsSNARE protein CsTYN11 (CsaV4_5G000834) with 121.5 kDa and CsTYN12 (CsaV4_3G000037) with 116.6 kDa, which were above the range. To investigate evolutionary dynamics, a comprehensive phylogenetic analysis was performed integrating *CsSNARE* sequences with their Arabidopsis and *O. sativa* counterparts (Figure 1). This analysis resolved the *CsSNARE* family into five discrete clades: *Qa-CsSNARE* (14 members), *Qb-CsSNARE* (9 members), *Qc-CsSNARE* (10 members), *Qb+c-CsSNARE* (3 members), and *R-CsSNARE* (15 members). The classification scheme aligns with established SNARE complex composition principles (Zhang et al., 2020), providing a framework for functional characterization of these key regulators in vesicle trafficking.

Table 1. Detailed information for *CsSNARE* genes in *C. sativus* L.

bioRxiv preprint doi: https://doi.org/10.64898/2026.03.30.715073; this version posted April 1, 2026. The copyright holder for this preprint (which was not certified by peer review) is the author/funder, who has granted bioRxiv a license to display the preprint in perpetuity. It is made available under a CC-BY 4.0 International license.

Gene Id	Genome position		Chr	Classification	Mw(KDa)	PI	Orthologous gene ID of *A. thaliana* and *O.sativa*	Gene name
	Start	End						
CsaV4_7G002084	25364812	25368886	Chr7	Qa-SNARE	27.3	7.93	*AT4G02195*	*CsSYP41*
CsaV4_6G003480	34473026	34473943	Chr6	Qa-SNARE	34.9	6.99	*AT2G18260*	*CsSYP112*
CsaV4_6G002929	30891676	30892872	Chr6	Qa-SNARE	34.8	7.76	*AT3G11820*	*CsSYP121*
CsaV4_6G000164	1077049	1080429	Chr6	Qa-SNARE	35.5	5.91	*AT1G51740*	*CsSYP81*
CsaV4_5G000808	5937809	5940766	Chr5	Qa-SNARE	24.2	9.23	*AT5G05760*	*CsSYP31*
CsaV4_4G001196	12306163	12307566	Chr4	Qa-SNARE	14.5	8.78	*AT1G08560*	*CsSYP111*
CsaV4_3G004278	39698225	39722061	Chr3	Qa-SNARE	21.9	9.08	*AT5G08080*	*CsSYP132*
CsaV4_3G003730	35942414	35944608	Chr3	Qa-SNARE	34.8	7.12	*AT3G52400*	*CsSYP122*
CsaV4_3G000157	1888929	1892532	Chr3	Qa-SNARE	30.2	5.7	*AT5G16830*	*CsSYP21*
CsaV4_2G003467	49450167	49458580	Chr2	Qa-SNARE	35.6	4.95	*Os07t0528900*	*CsSYP131a*
CsaV4_2G003466	49444610	49448216	Chr2	Qa-SNARE	19.5	9.52	*Os07t0528900*	*CsSYP131b*
CsaV4_2G003095	46733355	46738751	Chr2	Qa-SNARE	37.5	9.08	*AT3G24350*	*CsSYP32*
CsaV4_2G000481	4002763	4006503	Chr2	Qa-SNARE	26.3	6.36	*AT3G05710*	*CsSYP42*
CsaV4_1G001259	8380744	8382668	Chr1	Qa-SNARE	34.4	6.12	*AT4G03330*	*CsSYP123*
CsaV4_5G002760	31558825	31560998	Chr5	Qb+c-SNARE	33.1	5.87	*AT1G13890*	*CsSNAP30*
CsaV4_1G000627	4789002	4791123	Chr1	Qb+c-SNARE	32.7	6.43	*Os02t0437200*	*CsSNAP31*
CsaV4_1G000290	2771560	2775488	Chr1	Qb+c-SNARE	34.1	7.17	*AT5G07880*	*CsSNAP29*
CsaV4_6G000871	6883355	6887179	Chr6	Qb-SNARE	11.1	9.68	*AT3G24315*	*CsSEC20*
CsaV4_6G000020	172818	179777	Chr6	Qb-SNARE	16.7	5.56	*AT1G48240*	*CsNPSN12*

bioRxiv preprint doi: https://doi.org/10.64898/2026.03.30.715073; this version posted April 1, 2026. The copyright holder for this preprint (which was not certified by peer review) is the author/funder, who has granted bioRxiv a license to display the preprint in perpetuity. It is made available under a CC-BY 4.0 International license.

CsaV4_5G003292	35133085	35136577	Chr5	Qb-SNARE	23.7	6.32	*AT5G39510*	*CsVTI11*
CsaV4_5G000738	5343302	5346109	Chr5	Qb-SNARE	11.2	9.86	*Os01t0707300*	*CsVTI12*
CsaV4_4G002524	40922289	40929843	Chr4	Qb-SNARE	14.9	10.45	*AT2G45200*	*CsGOS12*
CsaV4_4G001166	12017759	12020620	Chr4	Qb-SNARE	26.2	9.61	*Os03t0655200*	*CsMEMB11*
CsaV4_4G000218	3539014	3544933	Chr4	Qb-SNARE	25.6	7.89	*AT1G15880*	*CsGOS11*
CsaV4_3G001260	10101433	10106837	Chr3	Qb-SNARE	26.6	5.83	*AT1G54110*	*CsUSE11*
CsaV4_3G000226	2495556	2501479	Chr3	Qb-SNARE	29.3	6.25	*AT2G35190*	*CsNPSN11*
CsaV4_7G001143	15949715	15952055	Chr7	Qc-SNARE	16.3	10.36	*AT1G16240*	*CsSYP51*
CsaV4_6G001777	20788623	20791473	Chr6	Qc-SNARE	30.2	5.11	*AT3G45280*	*CsSYP72*
CsaV4_6G000641	5313421	5317435	Chr6	Qc-SNARE	12.5	8.43	*Os08t0244100*	*CsSYP62*
CsaV4_3G004773	43718796	43721755	Chr3	Qc-SNARE	15.2	9.46	*AT4G14600*	*CsSFT11*
CsaV4_3G004097	38368888	38376475	Chr3	Qc-SNARE	34.9	8.30	*Os08t0244100*	*CsSYP61*
CsaV4_3G003487	34504356	34508388	Chr3	Qc-SNARE	30.1	5.23	*AT3G61450*	*CsSYP73b*
CsaV4_3G002908	30760524	30764050	Chr3	Qc-SNARE	30.1	5.23	*AT3G61450*	*CsSYP73a*
CsaV4_3G002476	22859134	22862516	Chr3	Qc-SNARE	15.3	8.82	*Os02t0820700*	*CsBET11*
CsaV4_3G002352	21179525	21182330	Chr3	Qc-SNARE	10.9	9.30	*Os09t0359700*	*CsSYP71*
CsaV4_3G000478	4588435	4591960	Chr3	Qc-SNARE	26.1	8.80	*Os02t0119400*	*CsSYP52*
CsaV4_7G002566	28287949	28292244	Chr7	R-SNARE	17.1	9.54	*AT1G11890*	*CsSEC221*
CsaV4_6G002654	28898152	28902838	Chr6	R-SNARE	25.0	9.16	*AT5G22360*	*CsVAMP713*
CsaV4_6G001541	12860107	12862878	Chr6	R-SNARE	15.8	9.54	*Os07t0249200*	*CsVAMP723*
CsaV4_6G000431	3731311	3734529	Chr6	R-SNARE	19.9	5.34	*Os08t0558600*	*CsVAMP726*
CsaV4_5G000834	6327037	6341269	Chr5	R-SNARE	121.5	5.26	*AT5G05570*	*CsTYN11*

bioRxiv preprint doi: https://doi.org/10.64898/2026.03.30.715073; this version posted April 1, 2026. The copyright holder for this preprint (which was not certified by peer review) is the author/funder, who has granted bioRxiv a license to display the preprint in perpetuity. It is made available under a CC-BY 4.0 International license.

CsaV4_3G000037	1093424	1104355	Chr3	R-SNARE	116.6	7.77	*AT4G35560*	*CsTYN12*
CsaV4_3G004616	42544074	42546877	Chr3	R-SNARE	25.1	9.34	*Os02t0803600*	*CsVAMP711*
CsaV4_3G002963	31230883	31232541	Chr3	R-SNARE	12.1	5.14	*AT5G52270*	*CsSEC223*
CsaV4_3G002836	29933038	29935795	Chr3	R-SNARE	13.9	9.32	*AT1G32670*	*CsVAMP725*
CsaV4_3G001771	13582691	13584508	Chr3	R-SNARE	27.9	9.63	*AT5G52270*	*CsSEC222*
CsaV4_3G001168	9588211	9591812	Chr3	R-SNARE	11.8	9.10	*AT4G15780*	*CsVAMP724*
CsaV4_2G000931	9331914	9335640	Chr2	R-SNARE	23.4	8.85	*Os12t0639800*	*CsVAMP722*
CsaV4_1G003990	41009733	41021353	Chr1	R-SNARE	16.8	7.63	*Os12t0639800*	*CsVAMP721*
CsaV4_1G002244	24128018	24131191	Chr1	R-SNARE	18.1	6.20	*AT5G58060*	*CsYKT61*
CsaV4_1G002154	23213296	23217113	Chr1	R-SNARE	15.6	5.50	*Os06t0174400*	*CsVAMP712*

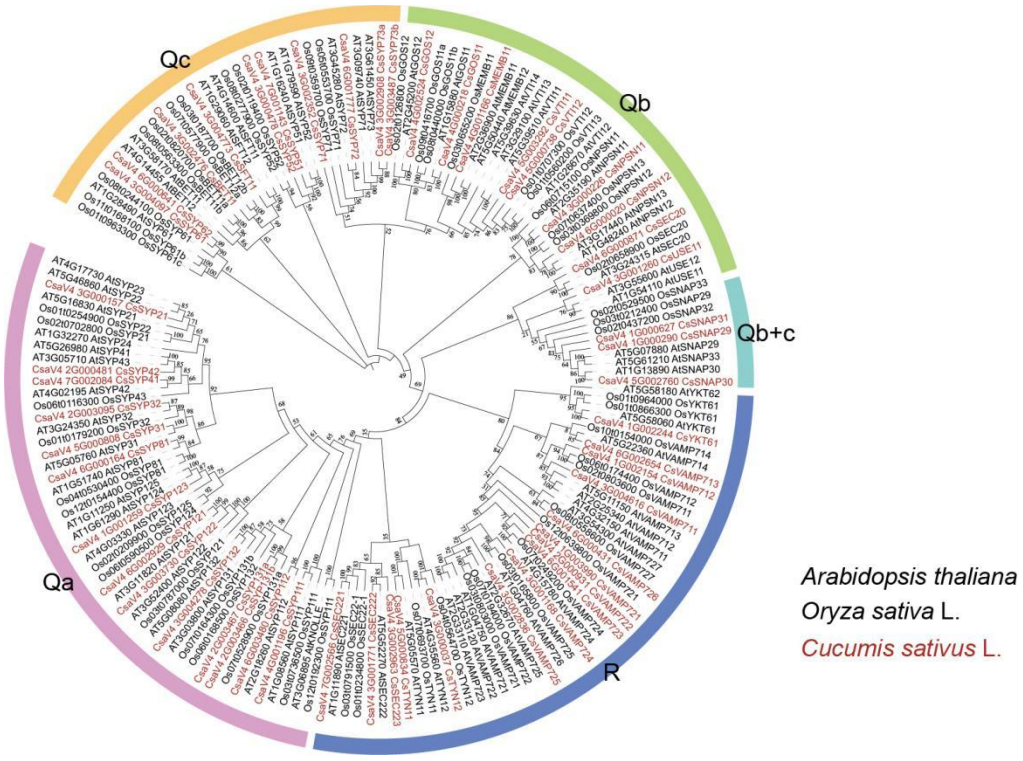

Fig. 1 Phylogenetic analysis of 51 *CsSNARE* genes identified in Cucumber. Different colours indicate different SNARE classifications.

bioRxiv preprint doi: https://doi.org/10.64898/2026.03.30.715073; this version posted April 1, 2026. The copyright holder for this preprint (which was not certified by peer review) is the author/funder, who has granted bioRxiv a license to display the preprint in perpetuity. It is made available under a CC-BY 4.0 International license.

3.2 Intrachromosomal distribution, exon-intron structure, conserved protein motifs, and cis-acting elements in the promoter region of CsSNARE genes

Figure 2 illustrates the non-random distribution pattern of *CsSNARE* genes across seven cucumber chromosomes. Notably, chromosome 3 emerged as the primary cluster with 18 *CsSNARE* genes, followed by chromosome 6 (10 genes) and chromosome 1 (6 genes). Chromosome 2 and 5 each harbored 5 *CsSNARE* genes. Chromosomes 4 and 7 each harbored 4 and 3 *CsSNARE* genes. This heterogeneous chromosomal localization suggests potential functional differentiation among *CsSNARE* genes.

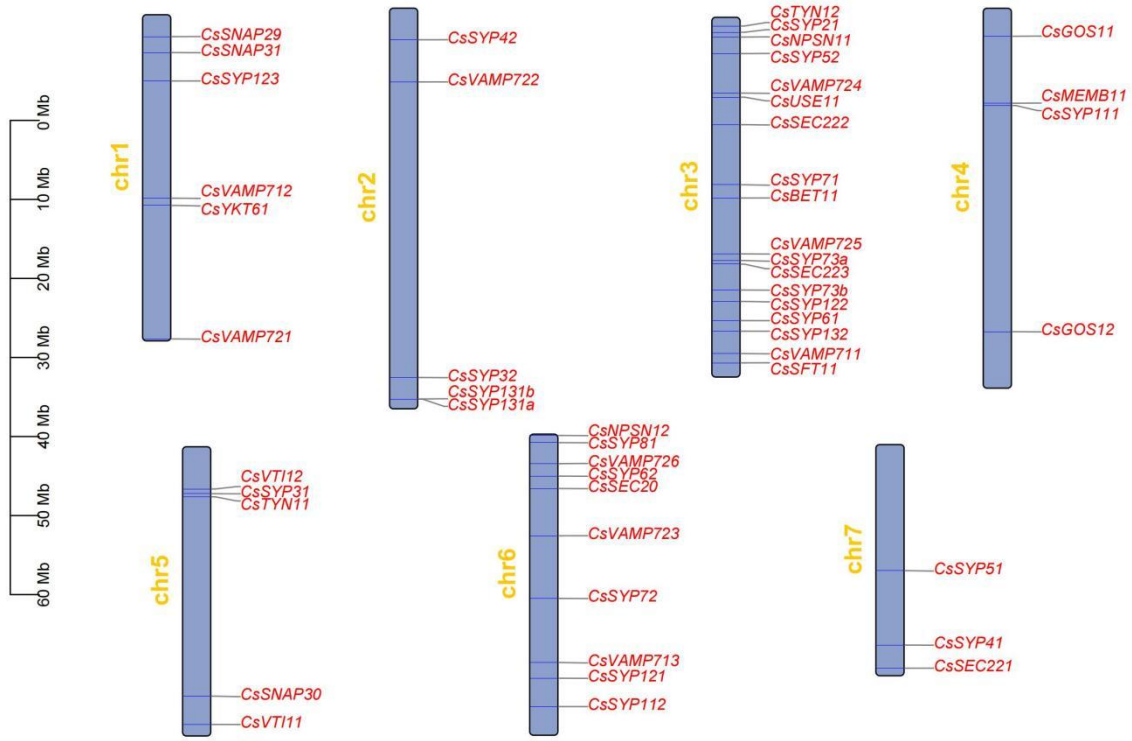

Fig. 2 Chromosomal distribution of *CsSNARE* genes in cucumber. The chromosomal locations of 51 *CsSNARE* genes were retrieved from the Cucumber Multi-omics Database (CLv4.0)

The exon-intron structures of *CsSNARE* genes are shown on the right side of Fig. 3. Except for *CsSYP21*, *CsSYP42*, *CsSYP81*, *CsSYP112*, *CsGOS11*, *CsSFT11* and *CsSYP61* which only contain coding sequences (CDS), other *CsSNARE* members all contain untranslated regions (UTR) and CDS. Members with closer kinship contain similar genetic structures.

bioRxiv preprint doi: https://doi.org/10.64898/2026.03.30.715073; this version posted April 1, 2026. The copyright holder for this preprint (which was not certified by peer review) is the author/funder, who has granted bioRxiv a license to display the preprint in perpetuity. It is made available under a CC-BY 4.0 International license.

Conserved motif characterization of CsSNARE proteins was conducted via the MEME suite, revealing 12 distinct conserved motifs across the family. As depicted in Figure 3 (left panel), motif distribution exhibited subfamily-specific patterns: R-CsSNARE members predominantly featured Motifs 2, 3, 4, 7, and 8; Qa-CsSNAREs uniquely harbored Motif 5; Qc-CsSNAREs co-expressed Motifs 1, 7, 8, 9, 10, 11, and 12; Qb-CsSNAREs contained Motifs 1, 6, and 11; while Qb+c-CsSNAREs exclusively retained Motif 1, 6, and 11. Notably, Except for R-CsSNARE, motif 1 is widespread in other subfamilies, implicating its potential role as a fundamental component of the CsSNARE core structure. Motif 5 localized to the N-terminal Habc domain in most Qa-CsSNAREs. The R-CsSNARE subgroup specifically enriched for Motifs 3 and 7, corresponding to the Longin domain (Motifs 2+8). Similar conserved motifs within the same subfamily indicate that they may have similar functions, while the different distributions of conserved motifs in different subfamilies may be one of the reasons for their functional diversity during the evolutionary process. These motif architectures corroborate the phylogenetic classification of CsSNARE proteins, reinforcing functional distinctions among subfamily members.

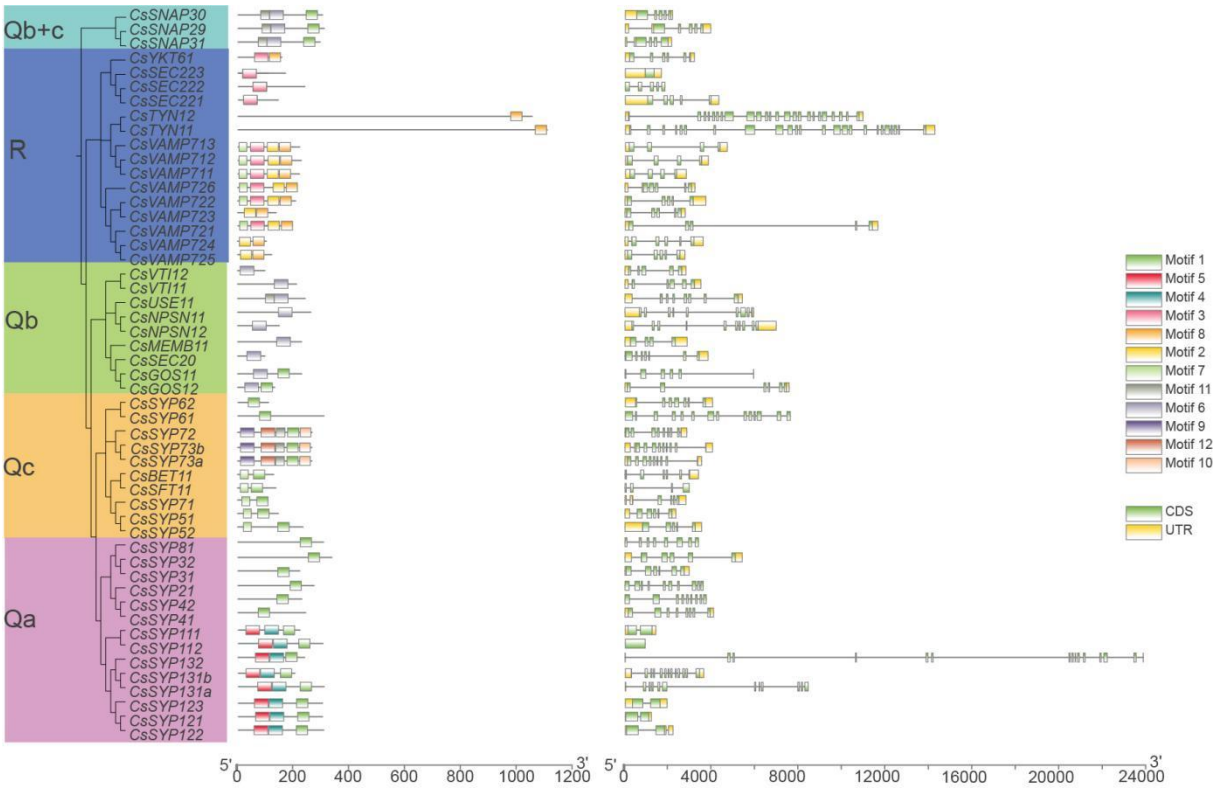

Fig. 3 Protein motifs and gene structures of *CsSNARE* from Cucumber. (Left) In the CsSNARE proteins, 12 motifs were identified by the MEME tool, represented by different colors (1-12) and depicted by TBtools. (Right) The exon-intron structure of these *CsSNARE* genes were predicted by

bioRxiv preprint doi: https://doi.org/10.64898/2026.03.30.715073; this version posted April 1, 2026. The copyright holder for this preprint (which was not certified by peer review) is the author/funder, who has granted bioRxiv a license to display the preprint in perpetuity. It is made available under a CC-BY 4.0 International license.

311 TBtools. The yellow boxes represent the coding sequence (CDS), the black lines represent introns, and
312 the green boxes represent up/downstream untranslated regions (UTR).
313
314 To understand how *CsSNARE* genes are regulated, we analyzed cis-acting elements (CREs) in the
315 2,000 bp region upstream of each gene. We identified 34 types of CREs and grouped them into three
316 main categories. Firstly, Light-Responsive Elements, including part of a conserved DNA module
317 involved in light responsiveness (182 occurrences, 18.5%), *cis*-acting regulatory element involved in
318 light responsiveness (115 occurrences, 11.7%), and part of a module for light response (28 occurrences,
319 2.8%). Second, Plant Hormone-Responsive Elements, including *cis*-acting regulatory element involved
320 in MeJA-responsiveness (120 occurrences, 12.2%), *cis*-acting element involved in abscisic acid
321 responsiveness (103 occurrences, 10.5%), *cis*-acting element involved in salicylic acid responsiveness
322 (33 occurrences, 3.4%), Gibberellin-responsive element (28 occurrences, 2.8%), Auxin-responsive
323 element (24 occurrences, 2.4%). Third, Stress-Responsive Elements, including *cis*-acting regulatory
324 element essential for anaerobic induction (117 occurrences, 11.9%), *cis*-acting element involved in
325 defense and stress responsiveness (34 occurrences, 3.5%), MYB binding site involved in
326 drought-inducibility (29 occurrences, 3.0%), *cis*-acting element involved in low-temperature
327 responsiveness (15 occurrences, 1.5%). Additionally, we found Auxiliary Regulatory Elements,
328 including *cis*-acting regulatory element involved in circadian control (10 occurrences), *cis*-acting
329 regulatory element involved in zein metabolism regulation (33 occurrences), *cis*-acting regulatory
330 element related to meristem expression (18 occurrences), and CRE involved in endosperm expression
331 (10 occurrences). The abundance of stress-related and hormone-responsive motifs suggests the
332 CsSNARE family helps plants respond to various stresses and hormones.

bioRxiv preprint doi: https://doi.org/10.64898/2026.03.30.715073; this version posted April 1, 2026. The copyright holder for this preprint (which was not certified by peer review) is the author/funder, who has granted bioRxiv a license to display the preprint in perpetuity. It is made available under a CC-BY 4.0 International license.

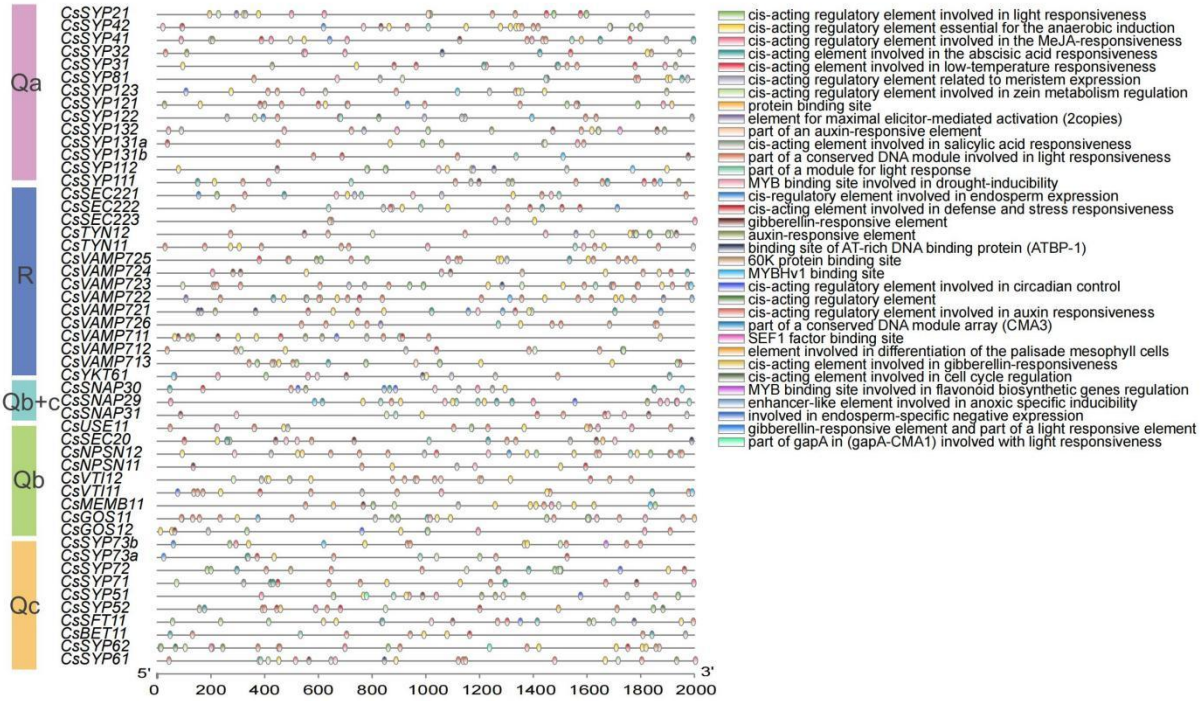

Fig. 4 *Cis*-acting element analysis of the promoter regions of *CsSNARE* genes in Cucumber. Based on the functional annotations, the cisacting elements were shown in boxes with different colors.

3.3 Intra- and inter-species covariance analysis of CsSNARE genes in cucumber

Next, we analyzed the evolutionary dynamics of *CsSNARE* gene duplication and identified conserved genomic regions across species. Through within-species comparative analysis of cucumber *CsSNARE* genes and interspecific synteny assessments with Arabidopsis and rice *SNARE* gene sets, key insights into genomic evolution were obtained. Figure 5A shows the chromosomal distribution of *CsSNARE* subfamilies (*CsSYPs*, *CsVAMPs*, *CsSNAPs*). This distribution suggests gene duplication drove family expansion. We identified seven segmental duplication events in cucumber. Chr3 was a hotspot, containing five events. Collinear gene pairs indicate possible functional similarities. Examples include: *CsVAMP724* on chromosome 3 is collinear with *CsVAMP725* on chromosome 3 and *CsVAMP722* on chromosome 2, and *CsSNAP30* on chromosome 5 is collinear with *CsSNAP29* and *CsSNAP31* on chromosome 1. It indicates that the *CsSNARE* gene may have undergone gene replication or gene drift, resulting in possible similarities in its function and expression pattern. This pattern implies segmental duplicative expansion as a major evolutionary force shaping the *CsSNARE*

bioRxiv preprint doi: https://doi.org/10.64898/2026.03.30.715073; this version posted April 1, 2026. The copyright holder for this preprint (which was not certified by peer review) is the author/funder, who has granted bioRxiv a license to display the preprint in perpetuity. It is made available under a CC-BY 4.0 International license.

gene family.

Synteny analysis revealed stronger conservation between cucumber and Arabidopsis (29 orthologous pairs) than between cucumber and rice (6 pairs). This reflects closer evolutionary relatedness between these dicots than between cucumber (dicot) and rice (monocot). These findings suggest distinct evolutionary paths shaped by lineage-specific duplications and selection.

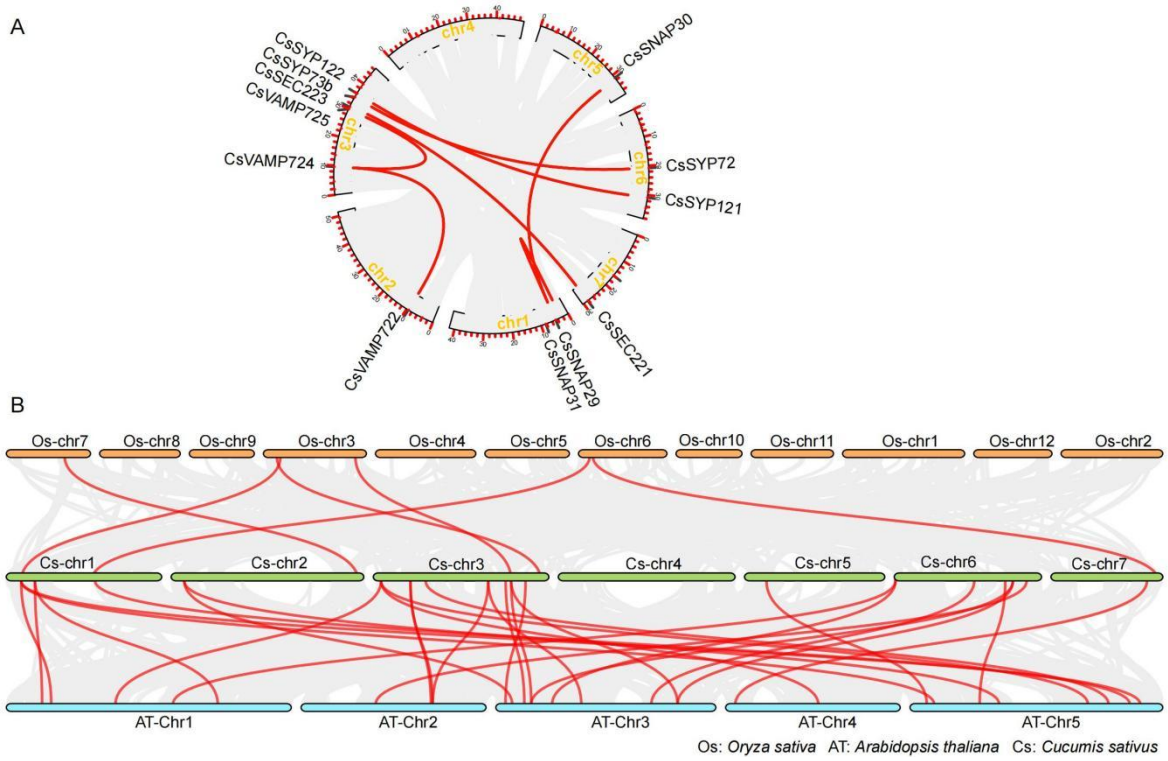

Fig.5 Intra- and inter-species covariance analysis of the *CsSNARE* gene family in Cucumber. (A) Collinearity analysis within the *CsSNARE* genes. (B) Collinearity analysis among *SNARE* genes. AT stands for *A. thaliana*, Cs for *C. sativus*, and Os for *O. sativa*. The *SNARE* gene pairs replicated in fragments are linked through red lines between chromosomes.

3.4 In silico transcript analysis of CsSNARE genes in cucumber

To understand *CsSNARE* functions, we analyzed their expression across tissues, organs, and developmental stages using public RNA-seq data. Figure 6 shows ubiquitous *CsSNARE* expression. Transcripts accumulated most in roots, hypocotyls, tendrils, and stems, suggesting key roles in vegetative growth and development. Within the *Qa-CsSNARE* subfamily, *CsSYP123* demonstrated remarkable upregulation in hypocotyl tissue, implicating its potential involvement in seedling

bioRxiv preprint doi: https://doi.org/10.64898/2026.03.30.715073; this version posted April 1, 2026. The copyright holder for this preprint (which was not certified by peer review) is the author/funder, who has granted bioRxiv a license to display the preprint in perpetuity. It is made available under a CC-BY 4.0 International license.

369 establishment and early growth regulation. Concurrently, *CsSYP121* displayed significant enrichment
370 in primary root tissues, potentially mediating fundamental processes such as ion uptake, nutrient
371 assimilation, and osmotic stress responses. The apical meristem-specific induction of *CsSYP112*,
372 *CsSYP41* and *CsSYP111* further supports its postulated function in governing morphogenic programs
373 and axial patterning during shoot development. Regarding leaf-specific expression, *Qc-CsSNARE*
374 member *CsSYP61* consistently exhibited elevated transcript abundance throughout leaf maturation
375 stages, indicating stage-specific regulatory functions potentially associated with foliar morphogenesis
376 or photosynthetic capacity development. These tissue- and stage-specific patterns highlight how
377 *CsSNARE* genes coordinate plant growth and adaptation.

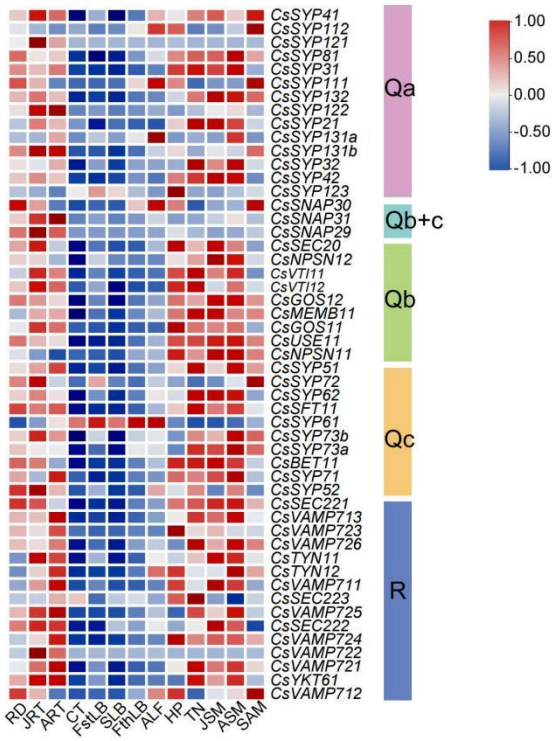

378

379 Fig. 6 Expression profile of *CsSNARE* genes in different tissues and developmental stages. RD is
380 radicle on juvenile, JRT is juvenile root, ART is Adult root, CT is Cotyledon, FstLB is first leaf blade,
381 SLB is second leaf blade, FthLB is forth leaf blade, ALF is Adult leaf, HP is Hypocotyl, TN is Tendril,
382 JSM is juvenile stem, ASM is Adult stem, SAM is Shoot apical meristem. The color scale represents
383 the level of expression (TPM value), from high (red) to low (blue). Gene expression data are
384 downloaded from the Cucumber Multi-omics database.

385

386 To elucidate the functional dynamics of the *CsSNARE* gene family under environmental stresses,

bioRxiv preprint doi: https://doi.org/10.64898/2026.03.30.715073; this version posted April 1, 2026. The copyright holder for this preprint (which was not certified by peer review) is the author/funder, who has granted bioRxiv a license to display the preprint in perpetuity. It is made available under a CC-BY 4.0 International license.

this study also retrieved transcriptomic profiling data (as TPM values) from the Cucumber Multi-omics Database. Figure 7 shows distinct expression patterns under different stresses. Most *CsSNARE* genes responded differentially to Angular Leaf Spot (ALS) and *Cladosporium cucumerinum* (CC) infections, indicating defense roles. During Gray Mold (GM), *CsSYP61* (*Qc-SNARE*) was uniquely induced, suggesting specific resistance to *Botrytis cinerea*. Most *R-CsSNARE* genes gradually increased during Powdery Mildew (PM) infection, suggesting sustained defense. Cold stress analysis unveiled complex regulatory patterns: *CsSYP123, CsVAMP721, CsNSPN11, CsNSPN12,* and *CsSNAP30* stayed constitutively high. *CsVAMP721* decreased during prolonged cold, suggesting negative feedback. *CsSYP122* and *CsSYP112* peaked at 24 hours. For heat stress, *CsSYP123* showed a transient peak at 20 minutes post-shock. *Qa-SNARE* genes dominated the heat response. Salt stress responsiveness analysis demonstrated temporally coordinated expression changes. *CsSYP132* rose continuously. Most genes peaked at 96 hours. *CsVAMP723*, *CsGOS11*, and *CsVTI12* responded early (48 hours). *CsSNAP30*, *CsSYP61*, *CsVAMP712*, and *CsUSE11* responded rapidly (within 10 hours).

Collectively, these dynamic expression profiles demonstrate widespread *CsSNARE* involvement in stress adaptation. They likely regulate membrane trafficking, cellular homeostasis, and stress signaling through precise temporal and tissue-specific mechanisms to enhance plant resilience.

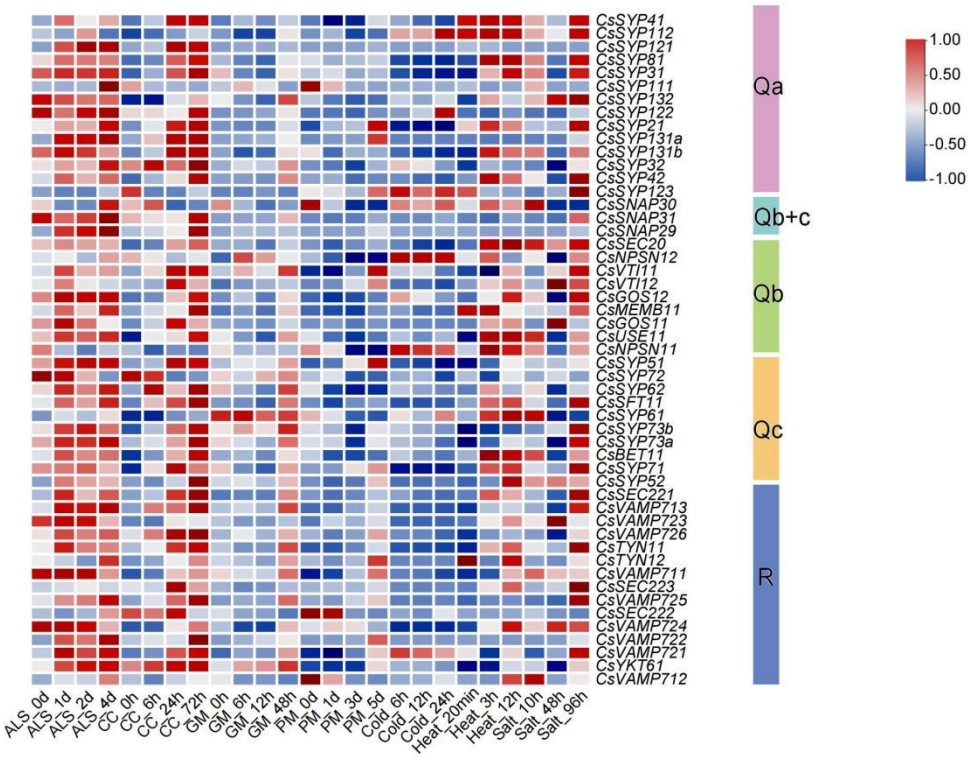

bioRxiv preprint doi: https://doi.org/10.64898/2026.03.30.715073; this version posted April 1, 2026. The copyright holder for this preprint (which was not certified by peer review) is the author/funder, who has granted bioRxiv a license to display the preprint in perpetuity. It is made available under a CC-BY 4.0 International license.

Fig. 7 The relative transcript levels of *CsSNARE* genes in Cucumber under different biological and abiotic stresses. ALS is angular leaf spot, CC is *Cladosporium cucumerium*, GM is Gray mold, PM is Powdery mildew. The color scale represents the level of expression (TPM value), from high (red) to low (blue). Gene expression data are downloaded from the Cucumber Multi-omics database.

3.5 Expression profles of CsSNARE genes in response to drought and salt stress

Integration of cis-acting element analyses within cucumber *CsSNARE* promoter regions (Fig. 5) and transcriptomic profiling under stress conditions (Fig. 7) indicated that the majority of *Qa-CsSNARE* genes are transcriptionally responsive to abiotic stresses. Building upon cucumber's known sensitivity to water deficit and salinity, we prioritized characterizing the drought response of this gene family. To mimic agricultural drought, plants were subjected to a 14-day withholding of irrigation. Subsequent qRT-PCR was employed to systematically resolve the expression dynamics of *Qa-CsSNARE* genes under these controlled conditions. As shown in Figure 8, after 14 days of drought stress, only *CsSYP41* exhibited significant upregulation compared to control plants. In contrast, *CsSYP81*, *CsSYP112*, *CsSYP122*, *CsSYP123*, *CsSYP131b*, and *CsSYP132* displayed significant downregulation at this final timepoint. Notably, the repression of *CsSYP112*, *CsSYP122*, and *CsSYP131b* began significantly earlier, at day 7 of treatment. While *CsSYP42* also showed significant downregulation at day 7, its expression recovered toward control levels by day 14.

To investigate salt stress responses, an experimental group was treated with a 150 mM NaCl solution, whereas the control group received standard cultivation practices. Leaf tissues were collected at 0, 3, and 7 days post-treatment for qRT-PCR analysis. The results revealed significant changes in the expression of *CsSYP21*, *CsSYP31*, *CsSYP32*, *CsSYP111*, *CsSYP122*, *CsSYP121*, *CsSYP123*, and *CsSYP131b* after 7 days of salinity (Fig. 9). Among these, *CsSYP121*, *CsSYP123*, and *CsSYP131b* were strongly induced, whereas the other genes were significantly repressed.

Initial analyses revealed constitutive high expression of *CsSYP121* in roots, as illustrated in Fig. 6. The response of *CsSYP121* expression in cucumber roots to salt stress was evaluated. Fig. S2 demonstrates that *CsSYP121* transcript abundance in roots increased significantly above control levels after 3 days of salt exposure, subsequently returning to baseline levels by day 7. Conversely, a marked and significant upregulation of *CsSYP121* expression was observed in leaves following 7 days of salt

bioRxiv preprint doi: https://doi.org/10.64898/2026.03.30.715073; this version posted April 1, 2026. The copyright holder for this preprint (which was not certified by peer review) is the author/funder, who has granted bioRxiv a license to display the preprint in perpetuity. It is made available under a CC-BY 4.0 International license.

435 treatment. Based on these findings, leaf-related phenotypic changes warrant focused attention in future
436 studies.
437

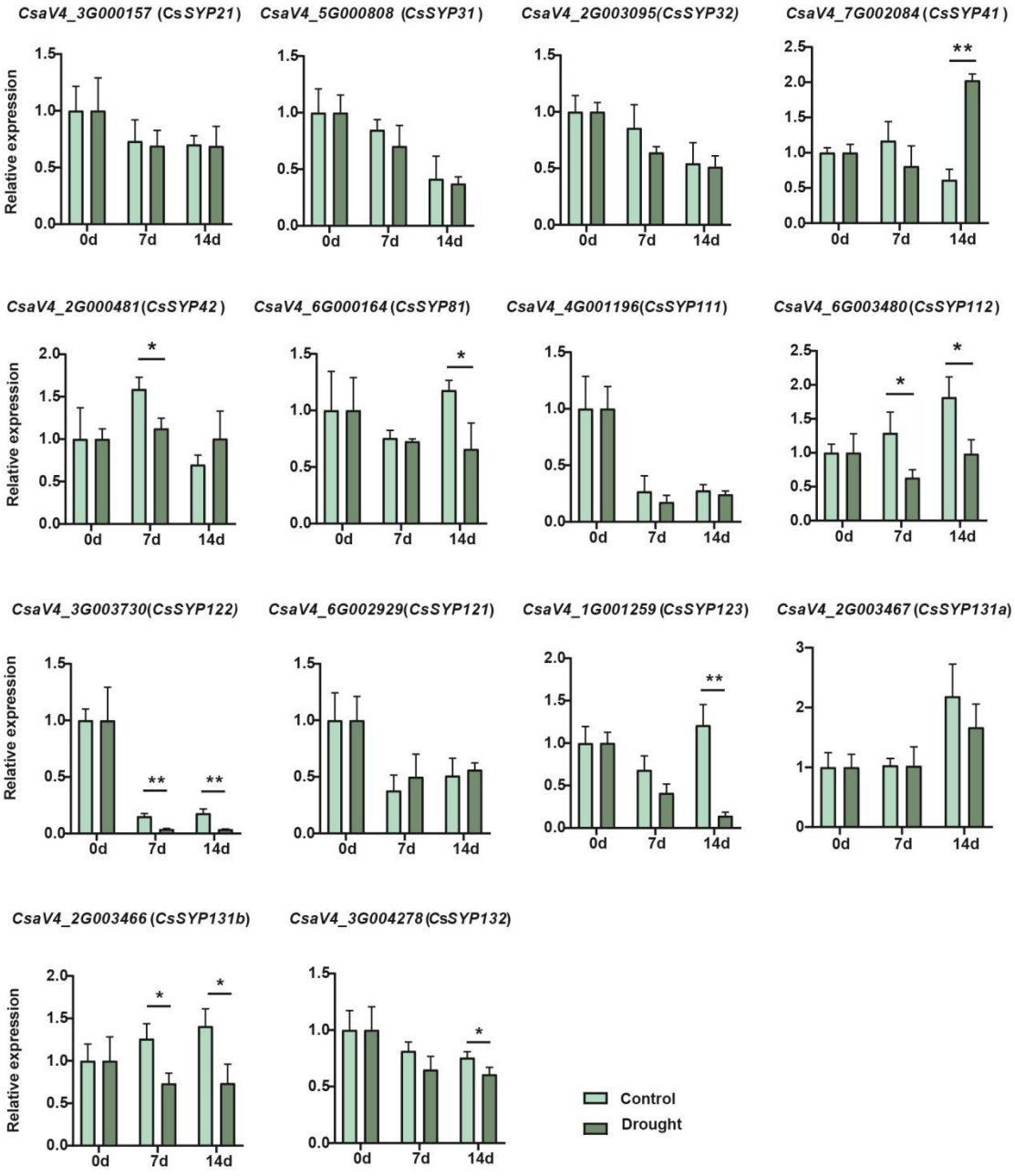

438

439 Fig. 8 Expression profiles of *Qa-CsSNARE* genes up-regulated or downregulated in Cucumber under
440 drought stress. The qRT-PCR analyses were used to access transcript levels of *Qa-CsSNARE* genes
441 with or without seven and fourteen days of drought treatment. Each bar represents the mean±SE
442 normalized to *CsEF1α* (*CsaV4_5G001996*) and *CsCACS* (*CsaV4_3G004932*). All samples were run in
443 three biological and three technical replicates. Light green columns represent "Control", and Dark
444 green columns represent "Drought". Asterisk indicates that the gene expression under stress has a

bioRxiv preprint doi: https://doi.org/10.64898/2026.03.30.715073; this version posted April 1, 2026. The copyright holder for this preprint (which was not certified by peer review) is the author/funder, who has granted bioRxiv a license to display the preprint in perpetuity. It is made available under a CC-BY 4.0 International license.

445 significant difference compared with the control (*P<0.05, **P<0.01).

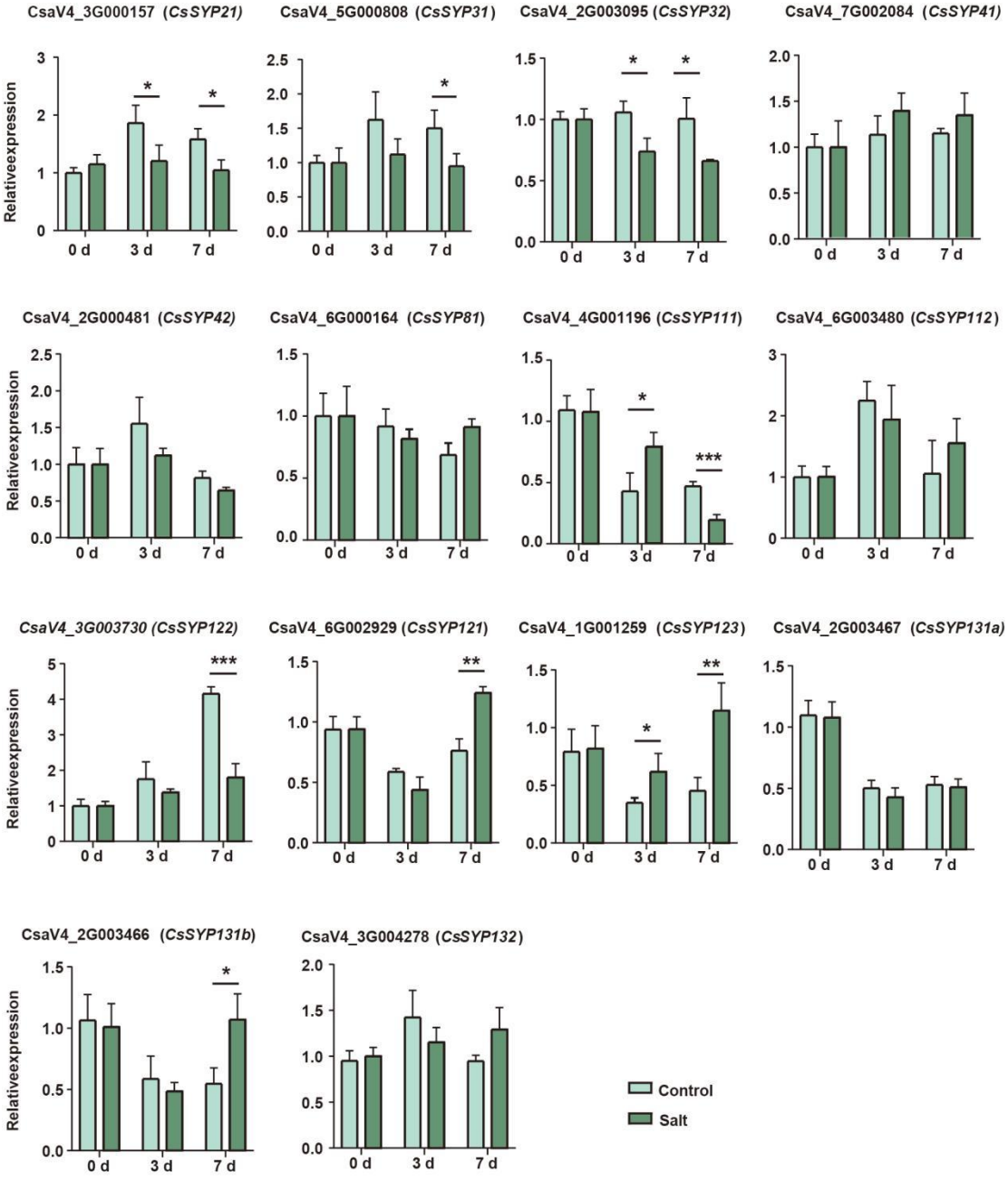

446

447 Fig. 9 Expression profiles of *Qa-CsSNARE* genes up-regulated or downregulated in wild-type
448 cucumbers under salt stress. The qRT-PCR analyses were used to access transcript levels of
449 *Qa-CsSNARE* genes with or without three and seven days of salt treatment. Each bar represents the
450 mean±SE normalized to *CsEF1α* (*CsaV4_5G001996*) and *CsCACS* (*CsaV4_3G004932*). All samples
451 were run in three biological and three technical replicates. Light green columns represent "Control",
452 and Dark green columns represent "Salt". Asterisk indicates that the gene expression after stress has a
453 significant difference compared with the control (*P<0.05, **P<0.01, ***P<0.001).

bioRxiv preprint doi: https://doi.org/10.64898/2026.03.30.715073; this version posted April 1, 2026. The copyright holder for this preprint (which was not certified by peer review) is the author/funder, who has granted bioRxiv a license to display the preprint in perpetuity. It is made available under a CC-BY 4.0 International license.

3.6 Overexpression of CsSYP121 alleviates the inhibitory effects of salt stress on cucumber by maintaining K^+ and Na^+ homeostasis and suppressing ROS accumulation

CsSYP121 is a member of the *Qa-SNARE* family in cucumber. It displays constitutive expression in most cucumber tissues, peaking in the root system (Fig. 6). No substantial changes in its transcript abundance were detected upon exposure to cold, heat, or drought stresses (Fig. 7-9). Moreover, after salt stress, the expression level of *CsSYP121* was significantly higher in both leaves and roots compared to the control group, with a more pronounced increase observed in the leaves (Fig. S2). Given that its ortholog in Arabidopsis and maize modulates plasma membrane K^+ channel and water channel activities via protein-protein interactions (Honsbein et al. 2009; Besserer et al. 2012; Hachez et al. 2014), we examined the physiological role of *CsSYP121* by overexpressing it in cucumber. The overexpression of *CsSYP121* was confirmed by qRT-PCR (Fig. S3) and western blot (Fig.S4). As shown in Figure 10, under control conditions, *CsSYP121* overexpression had no significant effect on plant height or stem diameter. After 7 days of salt stress treatment, inhibition of plant height and stem diameter was observed. However, *CsSYP121* overexpression alleviated the suppression of cucumber plant height. The 14-day drought stress treatment revealed that the *CsSYP121*-OE lines were as sensitive to drought stress as WT plant (Fig. S1). Combined with the qPCR results in Fig. 8, which showed that CsSYP121 was not significantly induced under drought stress, we speculate that this gene may functionally prioritize the regulation of ionic stress, with a relatively limited response to osmotic stress. Additionally, subcellular localization analysis of the CsSYP121 protein was performed, and the results showed that CsSYP121 co-localizes with the marker protein AtAHA1 at the plasma membrane (Fig. 10 E).

Next, we examined the effects of *CsSYP121* overexpression on water content and soluble solute content in cucumber plants under salt stress (Fig. 11). The results demonstrated that *CsSYP121* overexpression alleviated the increase in soluble solute content induced by salt stress. K^+ and Na^+, as critical inorganic salt ions, play vital roles in various key physiological processes, including osmoregulation in plants. In further experiments, we found that salt stress treatment resulted in increased Na^+ content and decreased K^+ content in the plants. However, *CsSYP121* overexpression effectively mitigated these alterations in ion levels. Within plant, ROS function as essential signaling

bioRxiv preprint doi: https://doi.org/10.64898/2026.03.30.715073; this version posted April 1, 2026. The copyright holder for this preprint (which was not certified by peer review) is the author/funder, who has granted bioRxiv a license to display the preprint in perpetuity. It is made available under a CC-BY 4.0 International license.

484 molecules. However, their pathological accumulation frequently acts as a primary contributor to
485 stress-elicited cellular damage. Consequently, strategies aimed at attenuating excessive ROS
486 accumulation constitute a fundamental defense mechanism during stress responses (Ali et al., 2023;
487 Foyer and Noctor, 2016). Enough K^+ supply is important for reducing ROS-related damage induced by
488 stress (Liu and Liao, 2022; Mostofa et al., 2022). Our prior work in foxtail millet demonstrated that
489 high potassium levels alleviated leaf ROS accumulation triggered by nanoplastic treatment (Guo et al.,
490 2024). Building upon these findings, we subsequently measured ROS levels and antioxidant enzyme
491 activities in cucumber. Under control conditions, *CsSYP121* overexpression exhibited no significant
492 effects H_2O_2 levels or antioxidant enzyme activities. Following salt stress imposition, wild-type plants
493 experienced a burst of ROS generation leading to injury. In contrast, *CsSYP121* overexpressing plants
494 displayed significantly enhanced antioxidant enzyme activity, which effectively counteracted the rise in
495 ROS levels.

bioRxiv preprint doi: https://doi.org/10.64898/2026.03.30.715073; this version posted April 1, 2026. The copyright holder for this preprint (which was not certified by peer review) is the author/funder, who has granted bioRxiv a license to display the preprint in perpetuity. It is made available under a CC-BY 4.0 International license.

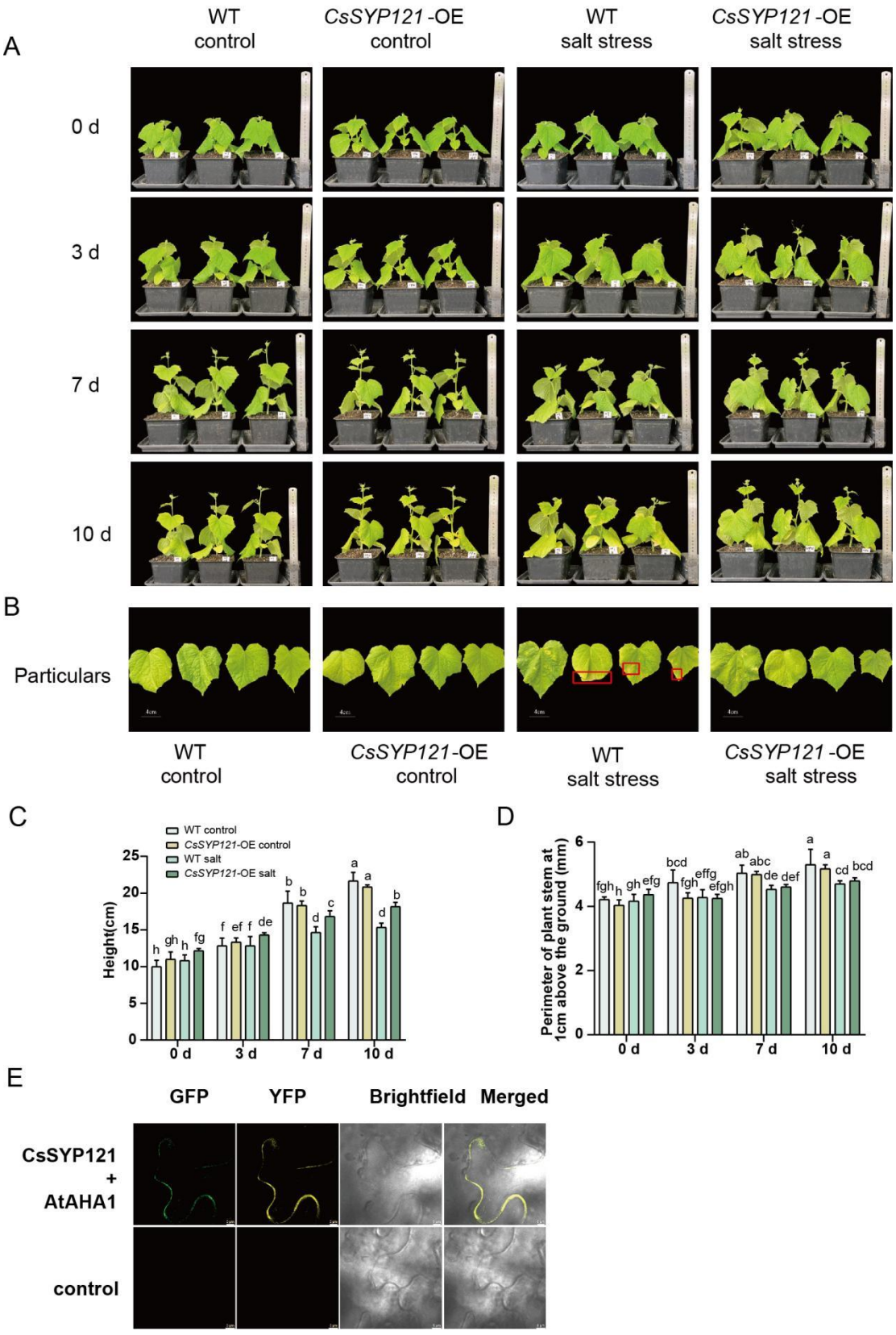

Fig. 10 Comparison of salt tolerance between *CsSYP121*-OE and wild-types cucumber plants. (A) The growth phenotypes of *CsSYP121*-OE and wild-types cucumber plants under salt stress of 0, 3 and 7 days. (B) The growth phenotypes and details of leaves of *CsSYP121*-OE and wild-types cucumber

bioRxiv preprint doi: https://doi.org/10.64898/2026.03.30.715073; this version posted April 1, 2026. The copyright holder for this preprint (which was not certified by peer review) is the author/funder, who has granted bioRxiv a license to display the preprint in perpetuity. It is made available under a CC-BY 4.0 International license.

plants under salt stress for 10 days. The red boxes indicate leaves with significant phenotypic differences. (C) The plant heights of *CsSYP121*-OE and wild-types cucumber plants under salt stress of 0, 3 and 7 days. (D) Stem thickness of *CsSYP121*-OE and wild-types cucumber plants under salt stress of 0, 3 and 7 days. (E) Subcellular localization of CsSYP121. Images from left to right are GFP fluorescence (CsSYP121), YFP fluorescence (AtAHA1), bright field, and merged field of view, respectively. Bright-field shows the tobacco cells. Merged image represents the overlay of the two channels. Scale bar = 5 μm. Results are from three independent experiments (biological replicates, n=3). Data points represent the mean of each independent experiment, with error bars showing SEM. Different letters indicate significant differences (P<0.05).

bioRxiv preprint doi: https://doi.org/10.64898/2026.03.30.715073; this version posted April 1, 2026. The copyright holder for this preprint (which was not certified by peer review) is the author/funder, who has granted bioRxiv a license to display the preprint in perpetuity. It is made available under a CC-BY 4.0 International license.

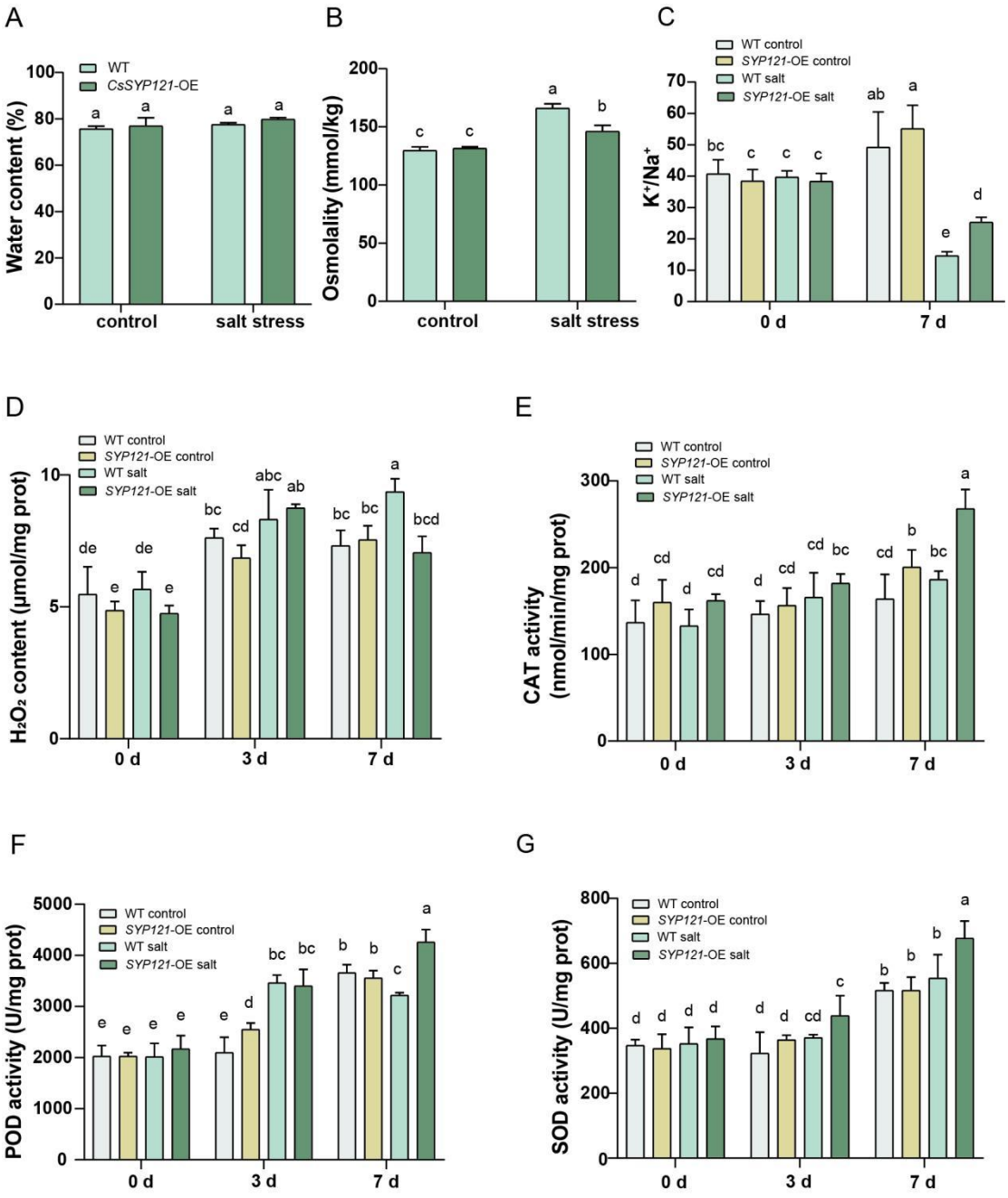

Fig. 11 The effects of salt stress on water content (A), osmotic pressure(B), K^+/Na^+ content ratios (C), H_2O_2 activity (D), CAT activity (E), POD activity (F), and SOD activity (G) of SYP121-OE and wild-type cucumbers. Results are from three independent experiments (biological replicates, n=3). Data points represent the mean of each independent experiment, with error bars showing SEM. Different letters indicate significant differences (P<0.05).

4. Discussion

Throughout their life cycles, plants routinely encounter various biotic and abiotic stresses.

bioRxiv preprint doi: https://doi.org/10.64898/2026.03.30.715073; this version posted April 1, 2026. The copyright holder for this preprint (which was not certified by peer review) is the author/funder, who has granted bioRxiv a license to display the preprint in perpetuity. It is made available under a CC-BY 4.0 International license.

519 Within plant systems, SNARE proteins represent a functionally diverse family exhibiting
520 multifaceted biological roles, particularly in responding to both biotic and abiotic challenges (Gu
521 et al., 2020; Zhang et al., 2020). Cucumber (*C. sativus* L.), as an agriculturally and nutritionally
522 valuable species, possesses considerable significance in horticulture, economy, and human
523 nutrition. In this study, we identified and characterized 51 members of the *CsSNARE* gene family
524 within the cucumber genome. Comprehensive bioinformatic analyses were performed to examine
525 their physicochemical characteristics, cis-acting elements, and expression patterns under abiotic
526 stress conditions. Furthermore, we investigated the function of *CsSYP121*-a member of the
527 *Qa-CsSNARE* subfamily-in salt stress responses through its overexpression in cucumber. Our
528 findings demonstrate that *CsSYP121* overexpression mitigates excessive ROS accumulation by
529 regulating K^+ and Na^+ levels, thereby contributing to cucumber's salt stress adaptation.

530 Drawing upon genetic data from Arabidopsis and rice, this study identified 51 putative
531 *CsSNARE* genes in cucumber—surpassing counts observed in algae (n=20), humans (n=35), and
532 yeast (n=24)-while approximating the complement size in foxtail millet (n=52) yet remaining
533 lower than that documented in Arabidopsis (n=65; Zhang et al. 2020). This expansion aligns with
534 evidence suggesting increased *SNARE* gene dosage correlates with enhanced multicellular
535 complexity during green plant evolution (Sanderfoot, 2007). Among these, we classified 14
536 *Qa-CsSNARE*, 9 *Qb-CsSNARE*, 10 *Qc-CsSNARE*, 3 *Qb+c-CsSNARE*, and 15 *R-CsSNARE*
537 members (Fig. 1). Such conserved categorization patterns underscore the fundamental role of
538 *SNARE* families in plant environmental adaptation. Comparative genomic analyses revealed
539 significantly more orthologous gene pairs between cucumber and Arabidopsis than between
540 cucumber and rice, attributable to their shared dicotyledonous lineage and correspondingly higher
541 sequence conservation (Soltis et al., 2019).

542 Tissue-specific expression profiling demonstrated distinct spatial regulation within the
543 *CsSNARE* family (Fig. 6). Notably, *Qa-CsSNARE* members including *CsSYP121*, *CsSYP41*,
544 *CsSYP131b*, and *CsSYP122* exhibited root-enriched transcript abundance, implicating roles in root
545 development—consistent with Arabidopsis *SYP121* function in root hair growth and functional
546 redundancy between SYP121/SYP122 paralogs (Waghmare et al. 2018). Our observation of
547 near-identical expression profiles for *CsSYP121* and *CsSYP122* across tissues supports this
548 redundancy hypothesis. Conversely, most *Qb-CsSNARE* genes displayed elevated expression in

bioRxiv preprint doi: https://doi.org/10.64898/2026.03.30.715073; this version posted April 1, 2026. The copyright holder for this preprint (which was not certified by peer review) is the author/funder, who has granted bioRxiv a license to display the preprint in perpetuity. It is made available under a CC-BY 4.0 International license.

meristematic and rapidly proliferating tissues (hypocotyls, seedling/adult stems, tendrils, shoot apex), mirroring the proliferation-associated expression pattern reported for *AtNSPN11* (Zheng et al., 2002) and suggesting potential functional overlap among family members. Distinctively, *Qc-CsSNARE CsSYP61* showed leaf-specific expression across developmental stages, coinciding with its proposed role in coordinating plant responses to carbon/oxygen dynamics (Hasegawa et al., 2022) and potentially regulating vegetative growth. Most members of the *R-CsSNARE* family exhibited higher expression levels in roots, stem, and shoot buds, while *CsVAMP722* and *CsSec223* were highly expressed across all tissues, including leaves. These collective findings validate our comprehensive identification of the *CsSNARE* gene family.

The cis-acting element analyses uncovered stress-responsive motifs (jasmonic acid responsive, low-temperature inducible, defense/stress-related) within *CsSNARE* promoters (Fig. 4). Prior studies have characterized specific SNARE complexes-such as the SYP121-SNAP33-VAMP721/722 complex-as components of Arabidopsis responses to biotic stresses (Kwon et al. 2008; Zhang et al. 2020). Analysis of publicly available RNA-Seq datasets revealed that most *CsSNARE* genes underwent rapid transcriptional activation within 24-48 hours following challenges by angular leaf spot pathogens and *C. cucumerium* infection. In contrast, Gray mold and Powdery mildew infections elicited elevated expression of these genes only after 3-5 days (Fig. 7), indicating functional diversification among *SNARE* family members during distinct biotic stress responses. Under abiotic stress conditions, heat and salt treatments broadly upregulated most *CsSNARE* genes, whereas cold stress induced significant expression changes in a subset comprising *CsSYP112*, *CsSYP122*, *CsSYP123*, *CsSNAP30*, *CsNPSN11*, *CsNPSN12*, and *CsVAMP721*.

SNARE proteins assume a central role in mediating plant responses to abiotic stressors-including drought, high salinity, and extreme temperatures (Pratelli et al., 2004). Through their function in membrane fusion, SNAREs facilitate the targeted transport of stress-responsive proteins, including antioxidant related proteins, to specific subcellular compartments, a process frequently accompanied by dynamic shifts in protein localization (Neves et al., 2021). In this study, promoter analysis of *CsSNARE* genes revealed that members of the *Qa-CsSNARE* subgroup harbor multiple cis-acting elements linked to drought responsiveness, including an MBS (MYB binding site) implicated in drought induction (Fig. 4). Consistent with

bioRxiv preprint doi: https://doi.org/10.64898/2026.03.30.715073; this version posted April 1, 2026. The copyright holder for this preprint (which was not certified by peer review) is the author/funder, who has granted bioRxiv a license to display the preprint in perpetuity. It is made available under a CC-BY 4.0 International license.

579 this regulatory architecture, experimental evidence confirmed that *Qa-CsSNAREs* exhibit
580 significant transcriptional activation under salt stress conditions (Fig. 5). Accordingly, our
581 investigation centers on characterizing the stress-resistant functions of *Qa-CsSNAREs* in cucumber.
582 Notably, *CsSYP41* displayed significant upregulation exclusively under drought stress, with
583 minimal response to salt treatment (Fig. 8, 9). Supporting a functional role for SYP4 family
584 members in stress adaptation, previous studies documented growth inhibition in *syp4* double
585 mutants under osmotic and salt stress regimes (Uemura et al., 2012), proposing a mechanism
586 involving protein complex formation. In contrast, *CsSYP121* expression remained largely unchanged
587 under drought but showed marked upregulation under salt stress (Fig. 8, 9). Overexpression of
588 *CsSYP121* did not confer discernible phenotypic alterations under drought conditions compared to
589 wild-type plants (Fig. S1). Based on combined phenotypic and gene expression analyses under both
590 stresses, we hypothesize that *CsSYP121* operates beyond general osmotic stress regulation, potentially
591 modulating ionic homeostasis specifically under salt stress—a notion aligned with findings from
592 previous reports(Eisenach et al. 2012; Besserer et al. 2012) . Further research is warranted to elucidate
593 the signaling specificity underlying these distinct responses.

594 As a characterized ABA-responsive Qa-SNARE involved in stomatal regulation (Eisenach et
595 al., 2012; Leyman et al., 1999), SYP121 emerged as a candidate regulator of salt stress responses
596 in our study. We observed a significant induction of *CsSYP121* expression in cucumber leaves at 7
597 days post-salt treatment (Fig. 9). To test its functionality, we generated *CsSYP121*-overexpressing
598 lines, which displayed enhanced salt tolerance compared to wild-type controls (Fig. 10). This
599 result aligns with findings from soybean (Hong et al., 2022), where SYP121 was proposed to play
600 a positive role in salt stress acclimation. These results reinforce a broader theme: manipulating
601 SNARE-mediated membrane traffic appears to be a conserved strategy for improving salt
602 tolerance across species, as evidenced by the effects of *GsSNAP33*, *AtSFT12*, and *SlSLSP6*
603 overexpression (Nisa et al., 2017; Salinas-Cornejo et al., 2023; Tarte et al., 2015).

604 Our findings show that overexpression of *CsSYP121* has no significant impact on cucumber
605 growth (Fig. 10). By contrast, Arabidopsis-based analyses indicate that *SYP121* overexpression
606 confers a moderate enhancement to seedling development (Zhang et al., 2019), thereby
607 demonstrating functional divergence of this gene across plant species. Our data suggest a
608 complementary mechanism for *CsSYP121* function under salt stress. Previous research from

bioRxiv preprint doi: https://doi.org/10.64898/2026.03.30.715073; this version posted April 1, 2026. The copyright holder for this preprint (which was not certified by peer review) is the author/funder, who has granted bioRxiv a license to display the preprint in perpetuity. It is made available under a CC-BY 4.0 International license.

609 Arabidopsis links SYP121 directly to ionic homeostasis. Recessive *syp121* mutants exhibit salt
610 hypersensitivity due to impaired K^+/Na^+ balance (Eisenach et al., 2012). Molecularly, SYP121
611 partners with KC1 and AKT1 to promote K^+ uptake (Honsbein et al., 2009) and also interacts with
612 the KAT1 channel (Honsbein et al., 2011; Lefoulon et al., 2018). In our study, *CsSYP121*-OE
613 plants maintained significantly higher K^+ levels under salt stress (Fig. 11C) and reduced ROS
614 accumulation (Fig. 11D-G). Maintaining a high cytoplasmic K^+ concentration is crucial for
615 counteracting Na^+ toxicity, preserving enzymatic activity, and sustaining osmotic homeostasis
616 (Fang et al., 2021). High intracellular K^+ not only supports cell turgor but also helps counteract
617 Na^+ toxicity and reduces ROS accumulation (Che et al., 2024; Guo et al., 2024). Thus, *CsSYP121*
618 likely enhances salt tolerance by improving K^+/Na^+ homeostasis and reducing ROS damage.
619 Further studies are warranted to investigate potential interactions and regulatory relationships
620 between *CsSYP121*, cucumber K^+ channels, and Na^+ transporters.
621
622 **5. Conclusion**
623
624 This study employed a genome-wide research to identify 51 *CsSNARE* genes in cucumber.
625 Based on phylogenetic analysis, conserved motif characterization, and exon-intron structure, these
626 genes were classified into five distinct subfamilies. Transcript profiling across diverse tissues,
627 developmental stages, and stress treatments demonstrated that the *Qa-CsSNARE* subfamily is
628 highly responsive to abiotic stress. Further examination pinpointed *CsSYP121* as a positive
629 regulator of the salt stress response. To validate its function, we generated
630 *CsSYP121*-overexpressing lines, which exhibited significantly enhanced salt tolerance compared
631 to wild-type plants. Under salt stress, these transgenic plants showed improved ROS scavenging
632 capacity and K^+/Na^+ homeostasis. In summary, this study not only systematically elucidates the
633 evolutionary and expression characteristics of the *SNARE* gene family in cucumber but, more
634 importantly, preliminarily reveals the molecular mechanism by which CsSYP121 enhances salt
635 tolerance through the regulation of ion homeostasis and redox balance. This provides an important
636 candidate gene and theoretical foundation for breeding salt-tolerant cucumber varieties using gene
637 editing or molecular marker-assisted selection.
638

bioRxiv preprint doi: https://doi.org/10.64898/2026.03.30.715073; this version posted April 1, 2026. The copyright holder for this preprint (which was not certified by peer review) is the author/funder, who has granted bioRxiv a license to display the preprint in perpetuity. It is made available under a CC-BY 4.0 International license.

CRediT authorship contribution statement

Ben Zhang: Writing - review & editing, Supervision, Software, Methodology, Funding acquisition, Data curation. **Weijuan Zhou:** Writing - review & editing, Writing - original draft, Validation, Supervision, Methodology. **Jie Zheng:** Validation, Software, Methodology, Investigation, Data curation. **Shengjun Zhou:** Validation, Investigation. **Yue Guo:** Validation, Investigation. **Dongmei Kong:** Visualization, Software, Methodology. **Pu Yang:** Investigation, Formal analysis.

Declaration of Competing Interest

The authors declare that they have no known competing financial interests or personal relationships that could have appeared to influence the work reported in this paper.

Acknowledgements

We thank all the colleagues in our laboratory for providing useful discussions and technical assistance. This work was supported by the National Natural Science Foundation of China (No. 32272012), the Fund Program for the Scientific Activities of Selected Returned Overseas Professionals in Shanxi Province (No.20230003) to BZ. The funding bodies played no role in the design of the study and collection, analysis, and interpretation of data and in writing the manuscript.

Appendix A. Supporting information

Supplement table 1. Primers used in this study
Supplement table 2. Characteristics of the promoter region of *CsSNARE* genes in *Cucumis sativus* L.
Supplement Fig. S1 The phenotypes of *CsSYP121*-OE and wild-type cucumber plants after 14 days of drought
Supplement Fig. S2 Under salt stress, the expression level of the *CsSYP121* gene in the roots of wild-type cucumbers.
Supplement Fig. S3 The expression level of *CsSYP121*-OE plants was validated by qRT-PCR.
Supplement Fig. S4 Western blot analysis using the CsSYP121 antibody was performed to verify the overexpression of CsSYP121 at the protein level.

Data availability The datasets generated during and analysed during the current study are available from the corresponding author on reasonable request.

References

bioRxiv preprint doi: https://doi.org/10.64898/2026.03.30.715073; this version posted April 1, 2026. The copyright holder for this preprint (which was not certified by peer review) is the author/funder, who has granted bioRxiv a license to display the preprint in perpetuity. It is made available under a CC-BY 4.0 International license.

Ali, S., Tyagi, A., Bae, H., 2023. ROS interplay between plant growth and stress biology: Challenges and future perspectives. Plant Physiology and Biochemistry 203, 108032. https://doi.org/10.1016/j.plaphy.2023.108032

Bassham, D.C., Brandizzi, F., Otegui, M.S., Sanderfoot, A.A., 2008. The Secretory System of Arabidopsis. The Arabidopsis Book 6, e0116. https://doi.org/10.1199/tab.0116

Besserer, A., Burnotte, E., Bienert, G.P., Chevalier, A.S., Errachid, A., Grefen, C., Blatt, M.R., Chaumont, F., 2012. Selective Regulation of Maize Plasma Membrane Aquaporin Trafficking and Activity by the SNARE SYP121. Plant Cell 24, 3463–3481. https://doi.org/10.1105/tpc.112.101758

Cermesoni, C., Grefen, C., Ricardi, M.M., 2024. Where R-SNAREs like to roam - the vesicle-associated membrane proteins VAMP721 & VAMP722 in trafficking hotspots. Current Opinion in Plant Biology 81, 102571. https://doi.org/10.1016/j.pbi.2024.102571

Che, Y., Wang, H., Yao, T., Wang, Z., Bo, L., Zhang, H., 2024. Activation of the antioxidant system and transduction of the mediated by exogenous calcium improve drought resistance in tobacco. Plant Stress 13, 100551. https://doi.org/10.1016/j.stress.2024.100551

Chen, C., Wu, Y., Li, J., Wang, X., Zeng, Z., Xu, J., Liu, Y., Feng, J., Chen, H., He, Y., Xia, R., 2023. TBtools-II: A “one for all, all for one” bioinformatics platform for biological big-data mining. Molecular Plant 16, 1733–1742. https://doi.org/10.1016/j.molp.2023.09.010

Chen, Z., Wang, Y., Wang, J., Babla, M., Zhao, C., García-Mata, C., Sani, E., Differ, C., Mak, M., Hills, A., Amtmann, A., Blatt, M.R., 2016. Nitrate reductase mutation alters potassium nutrition as well as nitric oxide-mediated control of guard cell ion channels in *Arabidopsis*. New Phytologist 209, 1456–1469. https://doi.org/10.1111/nph.13714

Das, A., Kumari, K., Munshi, A.D., Raju, D., Talukdar, A., Singh, D., Hongal, D., Iquebal, M.A., Bhatia, R., Bhattacharya, R.C., Behera, T.K., Dey, S.S., 2024. Physio-chemical and molecular modulation reveals underlying drought resilience mechanisms in Cucumber (Cucumis sativus L.). Scientia Horticulturae 328, 112855. https://doi.org/10.1016/j.scienta.2024.112855

Eisenach, C., Chen, Z., Grefen, C., Blatt, M.R., 2012. The trafficking protein SYP121 of Arabidopsis connects programmed stomatal closure and K^+ channel activity with vegetative growth. The Plant Journal 69, 241–251. https://doi.org/10.1111/j.1365-313X.2011.04786.x

Enami, K., Ichikawa, M., Uemura, T., Kutsuna, N., Hasezawa, S., Nakagawa, T., Nakano, A., Sato, M.H., 2009. Differential Expression Control and Polarized Distribution of Plasma Membrane-Resident SYP1 SNAREs in Arabidopsis thaliana. Plant Cell Physiol 50, 280–289. https://doi.org/10.1093/pcp/pcn197

Fan, Y., Guo, Y., Zhang, H., Han, R., Yang, P., Liang, Z., Zhang, L., Zhang, B., 2024. Genome-wide identification of the MED25 BINDING RING-H2 PROTEIN gene family in foxtail millet (Setaria italica L.) and the role of SiMBR2 in resistance to abiotic stress in Arabidopsis. Planta 260, 22. https://doi.org/10.1007/s00425-024-04455-6

Fang, S., Hou, X., Liang, X., 2021. Response Mechanisms of Plants Under Saline-Alkali Stress. Front. Plant Sci. 12. https://doi.org/10.3389/fpls.2021.667458

Fasshauer, D., Sutton, R.B., Brunger, A.T., Jahn, R., 1998. Conserved structural features of the synaptic fusion complex: SNARE proteins reclassified as Q- and R-SNAREs. Proc. Natl. Acad. Sci. U.S.A. 95, 15781–15786. https://doi.org/10.1073/pnas.95.26.15781

bioRxiv preprint doi: https://doi.org/10.64898/2026.03.30.715073; this version posted April 1, 2026. The copyright holder for this preprint (which was not certified by peer review) is the author/funder, who has granted bioRxiv a license to display the preprint in perpetuity. It is made available under a CC-BY 4.0 International license.

717 Foyer, C.H., Noctor, G., 2016. Stress-triggered redox signalling: what's in pROSpect? Plant Cell &
718 Environment 39, 951–964. https://doi.org/10.1111/pce.12621
719 Gasteiger, E., 2003. ExPASy: the proteomics server for in-depth protein knowledge and analysis.
720 Nucleic Acids Research 31, 3784–3788. https://doi.org/10.1093/nar/gkg563
721 Grefen, C., Chen, Z., Honsbein, A., Donald, N., Hills, A., Blatt, M.R., 2010a. A novel motif essential
722 for SNARE interaction with the K(+) channel KC1 and channel gating in Arabidopsis. The
723 Plant cell 22, 3076–3092. https://doi.org/10.1105/tpc.110.077768
724 Grefen, C., Donald, N., Hashimoto, K., Kudla, J., Schumacher, K., Blatt, M.R., 2010b. A ubiquitin-10
725 promoter-based vector set for fluorescent protein tagging facilitates temporal stability
726 and native protein distribution in transient and stable expression studies: Fluorescence
727 tagging and expression in Arabidopsis. The Plant Journal 64, 355–365.
728 https://doi.org/10.1111/j.1365-313X.2010.04322.x
729 Grefen, C., Karnik, R., Larson, E., Lefoulon, C., Wang, Y., Waghmare, S., Zhang, B., Hills, A., Blatt,
730 M.R., 2015. A vesicle-trafficking protein commandeers Kv channel voltage sensors for
731 voltage-dependent secretion. Nature Plants 15108.
732 https://doi.org/10.1038/nplants.2015.108
733 Gu, X., Brennan, A., Wei, W., Guo, G., Lindsey, K., 2020. Vesicle Transport in Plants: A Revised
734 Phylogeny of SNARE Proteins. Evolutionary Bioinformatics 16, 1–11.
735 https://doi.org/doi.org/10.1177/1176934320956575
736 Guan, J., Miao, H., Zhang, Z., Dong, S., Zhou, Q., Liu, X., Beckles, D.M., Gu, X., Huang, S., Zhang, S.,
737 2024. A near-complete cucumber reference genome assembly and Cucumber-DB, a
738 multi-omics database. Molecular Plant 17, 1178–1182.
739 https://doi.org/10.1016/j.molp.2024.06.012
740 Guo, Y., Liu, L., Fan, Y., Du, S., Chen, Y., Duan, Y., Han, R., Xu, S., Wen, G., Zhou, W., Zhang, H., Yang,
741 P., Zhang, L., Liang, Z., Wang, Y., Zhang, B., 2024. Polyethylene terephthalate nanoplastics
742 affect potassium accumulation in foxtail millet (Setaria italica) seedlings. BMC Plant Biol
743 24, 1253. https://doi.org/10.1186/s12870-024-06007-2
744 Hachez, C., Laloux, T., Reinhardt, H., Cavez, D., Degand, H., Grefen, C., De Rycke, R., Inzé, D., Blatt,
745 M.R., Russinova, E., Chaumont, F., 2014. *Arabidopsis* SNAREs SYP61 and SYP121
746 Coordinate the Trafficking of Plasma Membrane Aquaporin PIP2;7 to Modulate the Cell
747 Membrane Water Permeability. The Plant Cell 26, 3132–3147.
748 https://doi.org/10.1105/tpc.114.127159
749 Hasegawa, Y., Huarancca Reyes, T., Uemura, T., Baral, A., Fujimaki, A., Luo, Y., Morita, Y., Saeki, Y.,
750 Maekawa, S., Yasuda, S., Mukuta, K., Fukao, Y., Tanaka, K., Nakano, A., Takagi, J., Bhalerao,
751 R.P., Yamaguchi, J., Sato, T., 2022. The TGN/EE SNARE protein SYP61 and the ubiquitin
752 ligase ATL31 cooperatively regulate plant responses to carbon/nitrogen conditions in
753 Arabidopsis. The Plant Cell 34, 1354–1374. https://doi.org/10.1093/plcell/koac014
754 Hong, W., 2005. SNAREs and traffic. Biochimica et Biophysica Acta (BBA) - Molecular Cell
755 Research 1744, 120–144. https://doi.org/10.1016/j.bbamcr.2005.03.014
756 Hong, Z., Li, Y., Zhao, Y., Yang, M., Zhang, X., Teng, Y., Jing, L., Kong, D., Liu, T., Li, S., Meng, F.,
757 Wang, Q., Zhang, L., 2022. Heterologous Expression of Arabidopsis AtARA6 in Soybean
758 Enhances Salt Tolerance. Front. Genet. 13. https://doi.org/10.3389/fgene.2022.849357
759 Honsbein, A., Blatt, M.R., Grefen, C., 2011. A molecular framework for coupling cellular volume
760 and osmotic solute transport control. Journal of Experimental Botany 62, 2363–2370.

bioRxiv preprint doi: https://doi.org/10.64898/2026.03.30.715073; this version posted April 1, 2026. The copyright holder for this preprint (which was not certified by peer review) is the author/funder, who has granted bioRxiv a license to display the preprint in perpetuity. It is made available under a CC-BY 4.0 International license.

https://doi.org/10.1093/jxb/erq386

Honsbein, A., Sokolovski, S., Grefen, C., Campanoni, P., Pratelli, R., Paneque, M., Chen, Z., Johansson, I., Blatt, M.R., 2009. A Tripartite SNARE-K+ Channel Complex Mediates in Channel-Dependent K+ Nutrition in *Arabidopsis*. The Plant Cell 21, 2859–2877. https://doi.org/10.1105/tpc.109.066118

Hu, B., Jin, J., Guo, A.-Y., Zhang, H., Luo, J., Gao, G., 2015. GSDS 2.0: an upgraded gene feature visualization server. Bioinformatics 31, 1296–1297. https://doi.org/10.1093/bioinformatics/btu817

Huang, S., Li, R., Zhang, Z., Li, L., Gu, X., Fan, W., Lucas, W.J., Wang, X., Xie, B., Ni, P., Ren, Yuanyuan, Zhu, H., Li, Jun, Lin, K., Jin, W., Fei, Z., Li, Guangcun, Staub, J., Kilian, A., Van Der Vossen, E.A.G., Wu, Y., Guo, J., He, J., Jia, Z., Ren, Yi, Tian, G., Lu, Y., Ruan, J., Qian, W., Wang, M., Huang, Q., Li, B., Xuan, Z., Cao, J., Asan, Wu, Z., Zhang, J., Cai, Q., Bai, Y., Zhao, B., Han, Y., Li, Ying, Li, X., Wang, S., Shi, Q., Liu, Shiqiang, Cho, W.K., Kim, J.-Y., Xu, Y., Heller-Uszynska, K., Miao, H., Cheng, Z., Zhang, S., Wu, J., Yang, Y., Kang, H., Li, M., Liang, H., Ren, X., Shi, Z., Wen, M., Jian, M., Yang, Hailong, Zhang, G., Yang, Z., Chen, R., Liu, Shifang, Li, Jianwen, Ma, L., Liu, H., Zhou, Y., Zhao, J., Fang, X., Li, Guoqing, Fang, L., Li, Yingrui, Liu, D., Zheng, Hongkun, Zhang, Y., Qin, N., Li, Z., Yang, G., Yang, S., Bolund, L., Kristiansen, K., Zheng, Hancheng, Li, Shaochuan, Zhang, X., Yang, Huanming, Wang, Jian, Sun, R., Zhang, B., Jiang, S., Wang, Jun, Du, Y., Li, Songgang, 2009. The genome of the cucumber, Cucumis sativus L. Nat Genet 41, 1275–1281. https://doi.org/10.1038/ng.475

Huisman, R., Hontelez, J., Mysore, K.S., Wen, J., Bisseling, T., Limpens, E., 2016. A symbiosis-dedicated SYNTAXIN OF PLANTS 13II isoform controls the formation of a stable host–microbe interface in symbiosis. New Phytologist 211, 1338–1351. https://doi.org/10.1111/nph.13973

Kanazawa, T., Era, A., Minamino, N., Shikano, Y., Fujimoto, M., Uemura, T., Nishihama, R., Yamato, K.T., Ishizaki, K., Nishiyama, T., Kohchi, T., Nakano, A., Ueda, T., 2016. SNARE molecules in Marchantia polymorpha: Unique and conserved features of the membrane fusion machinery. Plant and Cell Physiology 57, 307–324. https://doi.org/10.1093/pcp/pcv076

Karnik, R., Grefen, C., Bayne, R., Honsbein, A., Köhler, T., Kioumourtzoglou, D., Williams, M., Bryant, N.J., Blatt, M.R., 2013. Arabidopsis Sec1/Munc18 Protein SEC11 Is a Competitive and Dynamic Modulator of SNARE Binding and SYP121-Dependent Vesicle Traffic. Plant Cell 25, 1368–1382. https://doi.org/10.1105/tpc.112.108506

Karnik, R., Waghmare, S., Zhang, B., Larson, E., Lefoulon, C., Gonzalez, W., Blatt, M.R., 2017. Commandeering Channel Voltage Sensors for Secretion, Cell Turgor, and Volume Control. Trends in Plant Science 22, 81–95. https://doi.org/10.1016/j.tplants.2016.10.006

Kumar, S., Stecher, G., Li, M., Knyaz, C., Tamura, K., 2018. MEGA X: Molecular Evolutionary Genetics Analysis across Computing Platforms. Molecular Biology and Evolution 35, 1547–1549. https://doi.org/10.1093/molbev/msy096

Kwon, C., Lee, J.-H., Yun, H.S., 2020. SNAREs in Plant Biotic and Abiotic Stress Responses. Molecules and Cells 43, 501–508. https://doi.org/10.14348/molcells.2020.0007

Kwon, C., Neu, C., Pajonk, S., Yun, H.S., Lipka, U., Humphry, M., Bau, S., Straus, M., Kwaaitaal, M., Rampelt, H., Kasmi, F.E., Jürgens, G., Parker, J., Panstruga, R., Lipka, V., Schulze-Lefert, P., 2008. Co-option of a default secretory pathway for plant immune responses. Nature 451, 835–840. https://doi.org/10.1038/nature06545

bioRxiv preprint doi: https://doi.org/10.64898/2026.03.30.715073; this version posted April 1, 2026. The copyright holder for this preprint (which was not certified by peer review) is the author/funder, who has granted bioRxiv a license to display the preprint in perpetuity. It is made available under a CC-BY 4.0 International license.

Lefoulon, C., Waghmare, S., Karnik, R., Blatt, M.R., 2018. Gating control and K+ uptake by the KAT1 K+ channel leaveraged through membrane anchoring of the trafficking protein SYP121. Plant, Cell & Environment 41, 2668–2677. https://doi.org/10.1111/pce.13392

Lescot, M., Déhais, P., Thijs, G., Marchal, K., Moreau, Y., Van De Peer, Y., Rouzé, P., Rombauts, S., 2002. PlantCARE, a database of plant cis-acting regulatory elements and a portal to tools for in silico analysis of promoter sequences. Nucleic Acids Research 30, 325–327. https://doi.org/10.1093/nar/30.1.325

Leyman, B., Geelen, D., Quintero, F.J., Blatt, M.R., 1999. A Tobacco Syntaxin with a Role in Hormonal Control of Guard Cell Ion Channels. Science 283, 537–540. https://doi.org/10.1126/science.283.5401.537

Li, L., Du, L., Cao, Q., Yang, Z., Liu, Y., Yang, H., Duan, X., Meng, Z., 2023. Salt Tolerance Evaluation of Cucumber Germplasm under Sodium Chloride Stress. Plants 12, 2927. https://doi.org/10.3390/plants12162927

Liang, G., Han, R., Fan, J., Chen, Yue, Chen, Yuxiang, Gao, C., Guo, Y., Liang, Z., Yang, P., Zhang, H., Zhang, L., Zhang, B., 2024. Identification of SiEUL gene family in foxtail millet (Setaria italica L.) and the drought tolerance function of SiEULS3. Plant Growth Regul 104, 1629–1641. https://doi.org/10.1007/s10725-024-01246-7

Liu, C., Liao, W., 2022. Potassium signaling in plant abiotic responses: Crosstalk with calcium and reactive oxygen species/reactive nitrogen species. Plant Physiology and Biochemistry 173, 110–121. https://doi.org/10.1016/j.plaphy.2022.01.016

Liu, Haitao, Jiao, Q., Fan, L., Jiang, Y., Alyemeni, M.N., Ahmad, P., Chen, Y., Zhu, M., Liu, Haiping, Zhao, Y., Liu, F., Liu, S., Li, G., 2023. Integrated physio-biochemical and transcriptomic analysis revealed mechanism underlying of Si-mediated alleviation to cadmium toxicity in wheat. Journal of Hazardous Materials 452, 131366. https://doi.org/10.1016/j.jhazmat.2023.131366

Mostofa, M.G., Rahman, M.M., Ghosh, T.K., Kabir, A.H., Abdelrahman, M., Rahman Khan, M.A., Mochida, K., Tran, L.S.P., 2022. Potassium in plant physiological adaptation to abiotic stresses. Plant Physiology and Biochemistry 186, 279–289. https://doi.org/10.1016/j.plaphy.2022.07.011

Neves, J., Sampaio, M., Séneca, A., Pereira, S., Pissarra, J., Pereira, C., 2021. Abiotic Stress Triggers the Expression of Genes Involved in Protein Storage Vacuole and Exocyst-Mediated Routes. International Journal of Molecular Sciences 22, 10644. https://doi.org/10.3390/ijms221910644

Nisa, Z., Mallano, A.I., Yu, Y., Chen, C., Duan, X., Amanullah, S., Kousar, A., Baloch, A.W., Sun, X., Tabys, D., Zhu, Y., 2017. GsSNAP33 , a novel Glycine soja SNAP25-type protein gene: Improvement of plant salt and drought tolerances in transgenic Arabidopsis thaliana. Plant Physiology and Biochemistry 119, 9–20. https://doi.org/10.1016/j.plaphy.2017.07.029

Pratelli, R., Sutter, J.-U., Blatt, M.R., 2004. A new catch in the SNARE. Trends in Plant Science 9, 187–195. https://doi.org/10.1016/j.tplants.2004.02.007

Salinas-Cornejo, J., Madrid-Espinoza, J., Verdugo, I., Norambuena, L., Ruiz-Lara, S., 2023. A SNARE-like protein from Solanum lycopersicum increases salt tolerance by modulating vesicular trafficking in tomato. Front. Plant Sci. 14. https://doi.org/10.3389/fpls.2023.1212806

bioRxiv preprint doi: https://doi.org/10.64898/2026.03.30.715073; this version posted April 1, 2026. The copyright holder for this preprint (which was not certified by peer review) is the author/funder, who has granted bioRxiv a license to display the preprint in perpetuity. It is made available under a CC-BY 4.0 International license.

Sanderfoot, A., 2007. Increases in the Number of SNARE Genes Parallels the Rise of Multicellularity among the Green Plants. Plant Physiology 144, 6–17. https://doi.org/10.1104/pp.106.092973

Sogawa, A., Yamazaki, A., Yamasaki, H., Komi, M., Manabe, T., Tajima, S., Hayashi, M., Nomura, M., 2019. SNARE proteins LjVAMP72a and LjVAMP72b are required for root symbiosis and root hair formation in lotus japonicus. Frontiers in Plant Science 9, 1–11. https://doi.org/10.3389/fpls.2018.01992

Soltis, P.S., Folk, R.A., Soltis, D.E., 2019. Darwin review: angiosperm phylogeny and evolutionary radiations. Proc. R. Soc. B. 286, 20190099. https://doi.org/10.1098/rspb.2019.0099

Tarte, V.N., Seok, H.-Y., Woo, D.-H., Le, D.H., Tran, H.T., Baik, J.-W., Kang, I.S., Lee, S.-Y., Chung, T., Moon, Y.-H., 2015. Arabidopsis Qc-SNARE gene AtSFT12 is involved in salt and osmotic stress responses and Na+ accumulation in vacuoles. Plant Cell Rep 34, 1127–1138. https://doi.org/10.1007/s00299-015-1771-3

Uemura, T., Ueda, T., Nakano, A., 2012. The physiological role of SYP4 in the salinity and osmotic stress tolerances. Plant Signaling & Behavior 7, 1118–1120. https://doi.org/10.4161/psb.21307

Waghmare, S., Lileikyte, E., Karnik, R., Goodman, J.K., Blatt, M.R., Jones, A.M.E., 2018. SNAREs SYP121 and SYP122 Mediate the Secretion of Distinct Cargo Subsets. Plant Physiol. 178, 1679–1688. https://doi.org/10.1104/pp.18.00832

Waghmare, S., Xia, L., Ly, T.P., Xu, J., Farami, S., Burchmore, R., Blatt, M.R., Karnik, R., 2024. SYNTAXIN OF PLANTS 132 underpins secretion of cargoes associated with salicylic acid signaling and pathogen defense. Plant Physiology 189, 1639–1661. https://doi.org/10.1093/plphys/kiae541

Wang, G., Long, D., Yu, F., Zhang, H., Chen, C., Wang, Y., Ji, W., 2021. Genome-wide identification, evolution, and expression of the *SNARE* gene family in wheat resistance to powdery mildew. PeerJ 9, e10788. https://doi.org/10.7717/peerj.10788

Wang, H., Hao, D., Wang, X., Zhang, H., Yang, P., Zhang, L., Zhang, B., 2021. Genome-wide identification and expression analysis of the SNARE genes in Foxtail millet (Setaria italica) reveals its roles in drought stress. Plant Growth Regul 95, 355–369. https://doi.org/10.1007/s10725-021-00746-0

Wang, M., Jiang, B., Peng, Q., Liu, W., He, X., Liang, Z., Lin, Y., 2018. Transcriptome Analyses in Different Cucumber Cultivars Provide Novel Insights into Drought Stress Responses. IJMS 19, 2067. https://doi.org/10.3390/ijms19072067

Xia, L., Mar Marquès-Bueno, M., Bruce, C.G., Karnik, R., 2019. Unusual Roles of Secretory SNARE SYP132 in Plasma Membrane H^+ -ATPase Traffic and Vegetative Plant Growth. Plant Physiol. 180, 837–858. https://doi.org/10.1104/pp.19.00266

Xia, L., Mar Marquès-Bueno, M., Karnik, R., 2020. Trafficking SNARE SYP132 Partakes in Auxin-Associated Root Growth. Plant Physiol. 182, 1836–1840. https://doi.org/10.1104/pp.19.01301

Xu, J., Zhao, X., Bao, J., Shan, Y., Zhang, M., Shen, Y., Abubakar, Y.S., Lu, G., Wang, Z., Wang, A., 2022. Genome-Wide Identification and Expression Analysis of SNARE Genes in Brassica napus. Plants 11, 711. https://doi.org/10.3390/plants11050711

Xue, Y., Yang, Y., Yang, Z., Wang, X., Guo, Y., 2018. VAMP711 Is Required for Abscisic Acid-Mediated Inhibition of Plasma Membrane H^+ -ATPase Activity. Plant Physiol. 178,

bioRxiv preprint doi: https://doi.org/10.64898/2026.03.30.715073; this version posted April 1, 2026. The copyright holder for this preprint (which was not certified by peer review) is the author/funder, who has granted bioRxiv a license to display the preprint in perpetuity. It is made available under a CC-BY 4.0 International license.

1332–1343. https://doi.org/10.1104/pp.18.00499

Yano, D., Sato, M., Saito, C., Sato, M.H., Morita, M.T., Tasaka, M., 2003. A SNARE complex containing SGR3/AtVAM3 and ZIG/VTI11 in gravity-sensing cells is important for Arabidopsis shoot gravitropism. Proceedings of the National Academy of Sciences of the United States of America 100, 8589–8594. https://doi.org/10.1073/pnas.1430749100

Zeng, B., Zhou, X., Gou, H., Che, L., Lu, S., Yang, J., Cheng, Y., Liang, G., Mao, J., 2024. Molecular Evolution of SNAREs in Vitis vinifera and Expression Analysis under Phytohormones and Abiotic Stress. International Journal of Molecular Sciences 25, 5984. https://doi.org/10.3390/ijms25115984

Zhang, B., Guo, Y., Wang, H., Wang, X., Lv, M., Yang, P., Zhang, L., 2022. Identification and Characterization of Shaker K+ Channel Gene Family in Foxtail Millet (Setaria italica) and Their Role in Stress Response. Front. Plant Sci. 13, 907635. https://doi.org/10.3389/fpls.2022.907635

Zhang, B., Karnik, R., Alvim, J., Donald, N., Blatt, M.R., 2019. Dual Sites for SEC11 on the SNARE SYP121 Implicate a Binding Exchange during Secretory Traffic. Plant Physiol. 180, 228–239. https://doi.org/10.1104/pp.18.01315

Zhang, B., Karnik, R., Wang, Y., Wallmeroth, N., Blatt, M.R., Grefen, C., 2015. The Arabidopsis R-SNARE VAMP721 Interacts with KAT1 and KC1 K+ Channels to Moderate K+ Current at the Plasma Membrane. The Plant Cell 27, 1697–1717. https://doi.org/10.1105/tpc.15.00305

Zhang, B., Wang, H., Zhang, Y., 2020. SNARE proteins and their role in plant ion channel regulation. Plant Growth Regul 92, 443–453. https://doi.org/10.1007/s10725-020-00656-7

Zhang, C., Lyu, S., Gao, L., Song, X., Li, Y., Hou, X., 2018. Genome-Wide Identification, Classification, and Expression Analysis of SNARE Genes in Chinese Cabbage (Brassica rapa ssp. pekinensis) Infected by Turnip mosaic virus. Plant Molecular Biology Reporter 36, 210–224. https://doi.org/10.1007/s11105-017-1060-0

Zhang, L., Zhang, H., Liu, P., Hao, H., Jin, J.B., Lin, J., 2011. Arabidopsis R-SNARE proteins VAMP721 and VAMP722 are required for cell plate formation. PLoS ONE 6. https://doi.org/10.1371/journal.pone.0026129

Zheng, H., Bednarek, S.Y., Sanderfoot, A.A., Alonso, J., Ecker, J.R., Raikhel, N.V., 2002. NPSN11 Is a Cell Plate-Associated SNARE Protein That Interacts with the Syntaxin KNOLLE. Plant Physiology 129, 530–539. https://doi.org/10.1104/pp.003970

Zhou, Y., Sang, T., Tian, M., Jahan, M.S., Wang, J., Li, X., Guo, S., Liu, H., Wang, Y., Shu, S., 2022. Effects of Bacillus cereus on Photosynthesis and Antioxidant Metabolism of Cucumber Seedlings under Salt Stress. Horticulturae 8. https://doi.org/10.3390/horticulturae8050463

Zhu, J., Li, M., Lu, H., Li, Y., Ren, M., Xu, J., Ding, W., Wang, Y., Wu, Y., Liu, Y., Wu, Z., Mo, X., Mao, C., 2024. The t- SNARE protein OsSYP132 is required for vesicle fusion and root morphogenesis in rice. New Phytologist 244, 2413–2429. https://doi.org/10.1111/nph.20180

bioRxiv preprint doi: https://doi.org/10.64898/2026.03.30.715073; this version posted April 1, 2026. The copyright holder for this preprint (which was not certified by peer review) is the author/funder, who has granted bioRxiv a license to display the preprint in perpetuity. It is made available under a CC-BY 4.0 International license.

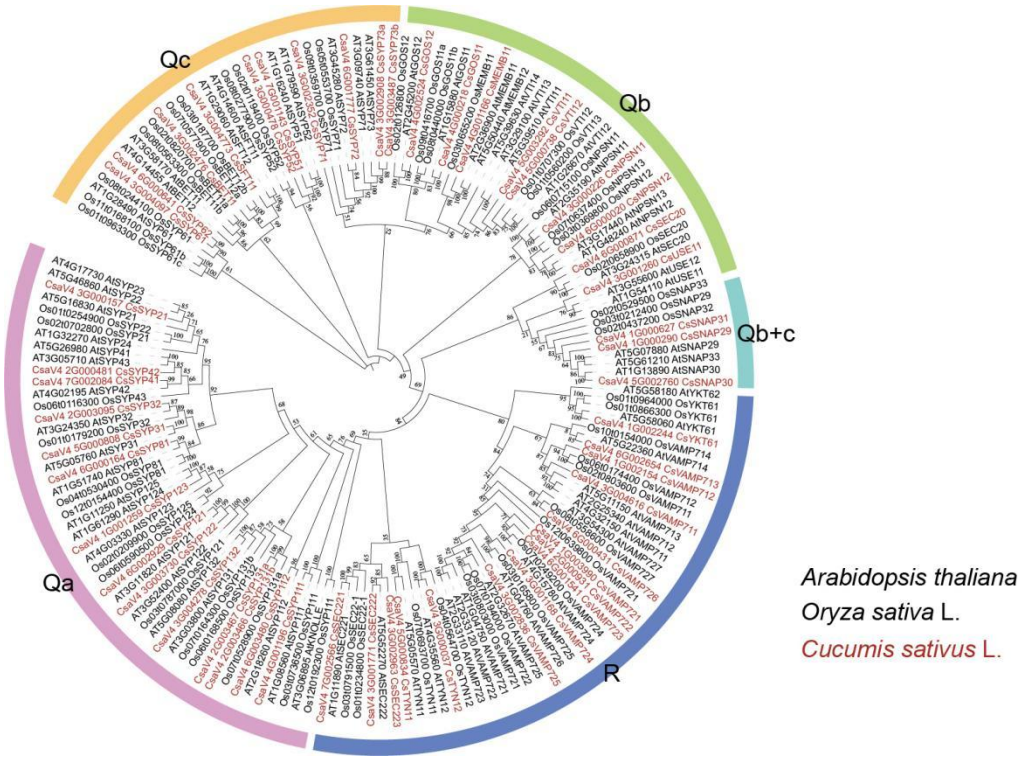

Fig. 1 Phylogenetic analysis of 51 *CsSNARE* genes identified in Cucumber. Different colours indicate different SNARE classifications.

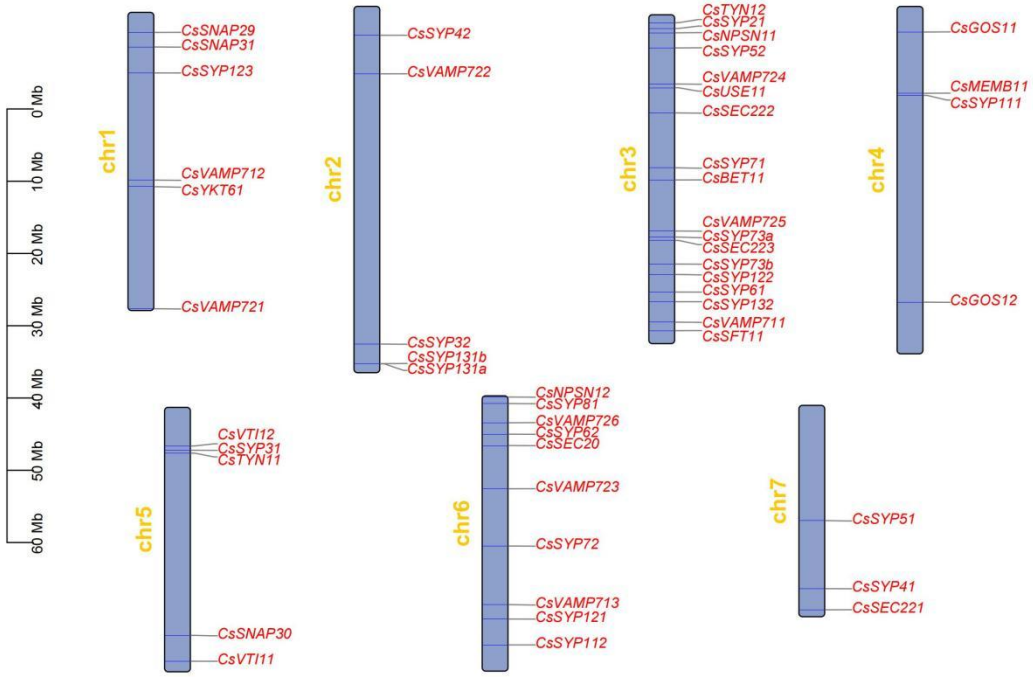

Fig. 2 Chromosomal localization of *CsSNARE* genes in Cucumber. The location information of 51 *CsSNARE* genes on the chromosome was obtained from the Cucumber Multi-omics database (CLv4.0)

bioRxiv preprint doi: https://doi.org/10.64898/2026.03.30.715073; this version posted April 1, 2026. The copyright holder for this preprint (which was not certified by peer review) is the author/funder, who has granted bioRxiv a license to display the preprint in perpetuity. It is made available under a CC-BY 4.0 International license.

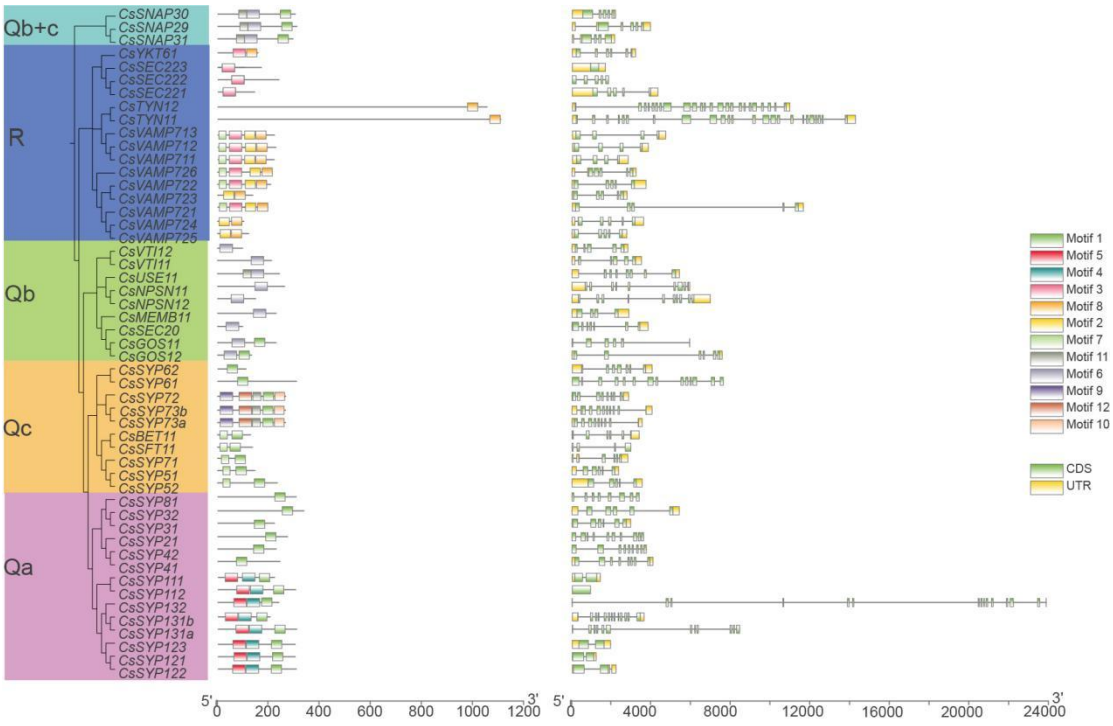

Fig. 3 Protein motifs and gene structures of *CsSNARE* from Cucumber. (Left) In the CsSNARE proteins, 12 motifs were identified by the MEME tool, represented by different colors (1-12) and depicted by TBtools. (Right) The exon-intron structure of these *CsSNARE* genes were predicted by TBtools. The yellow boxes represent the coding sequence (CDS), the black lines represent introns, and the green boxes represent up/downstream untranslated regions (UTR).

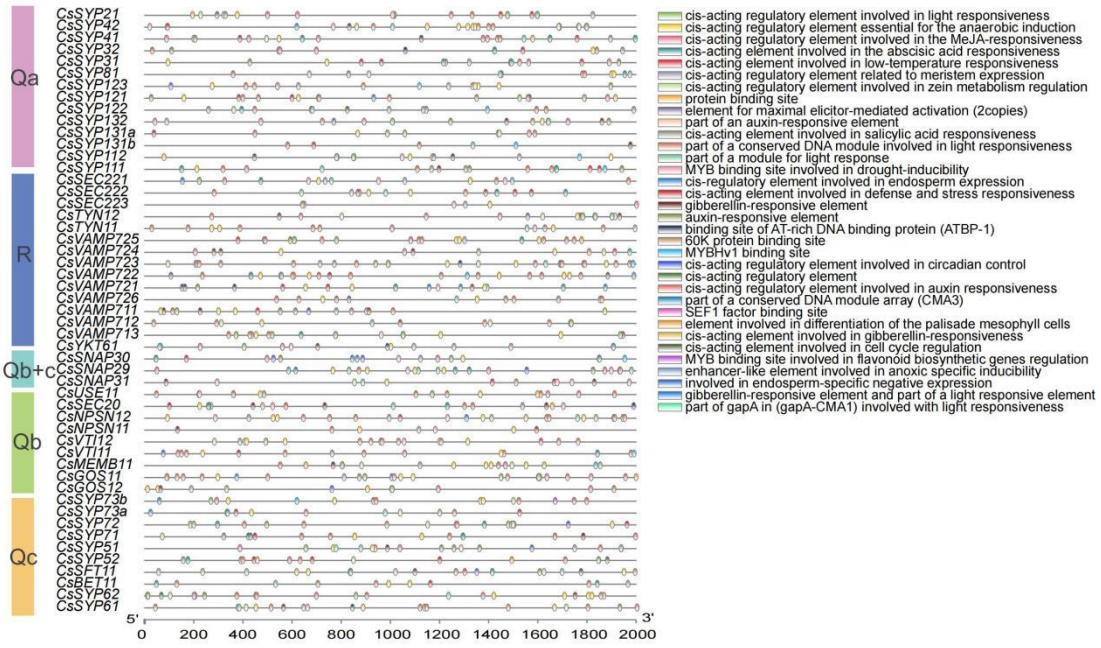

Fig. 4 *Cis*-acting element analysis of the promoter regions of *CsSNARE* genes in Cucumber. Based on

bioRxiv preprint doi: https://doi.org/10.64898/2026.03.30.715073; this version posted April 1, 2026. The copyright holder for this preprint (which was not certified by peer review) is the author/funder, who has granted bioRxiv a license to display the preprint in perpetuity. It is made available under a CC-BY 4.0 International license.

the functional annotations, the cisacting elements were shown in boxes with different colors.

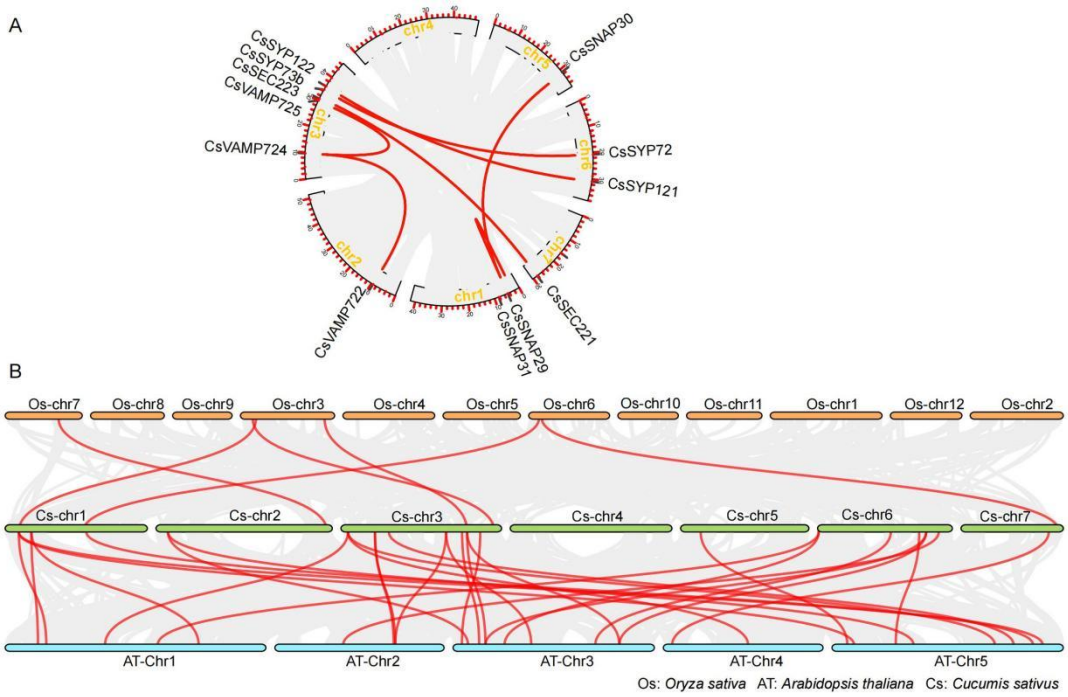

Fig.5 Intra- and inter-species covariance analysis of the *CsSNARE* gene family in Cucumber. (A) Collinearity analysis within the *CsSNARE* genes. (B) Collinearity analysis among *SNARE* genes. AT stands for *A. thaliana*, Cs for *C. sativus*, and Os for *O. sativa*. The *SNARE* gene pairs replicated in fragments are linked through red lines between chromosomes.

bioRxiv preprint doi: https://doi.org/10.64898/2026.03.30.715073; this version posted April 1, 2026. The copyright holder for this preprint (which was not certified by peer review) is the author/funder, who has granted bioRxiv a license to display the preprint in perpetuity. It is made available under a CC-BY 4.0 International license.

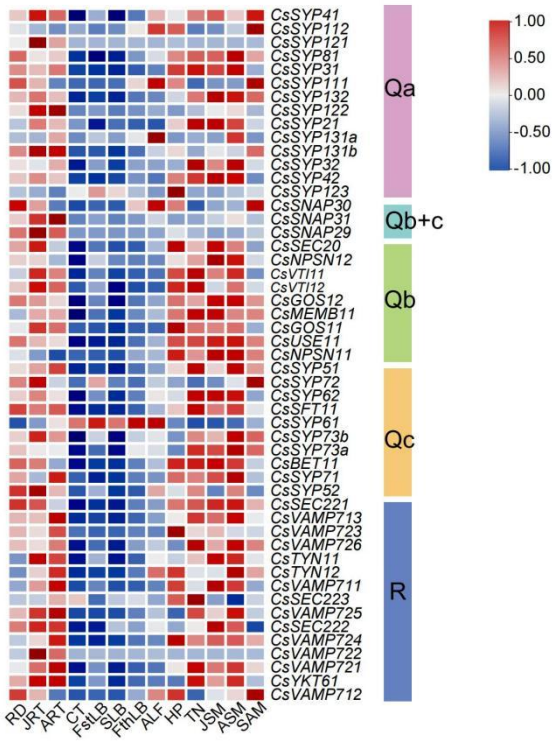

Fig. 6 Expression profile of *CsSNARE* genes in different tissues and developmental stages. RD is radicle on juvenile, JRT is juvenile root, ART is Adult root, CT is Cotyledon, FstLB is first leaf blade, SLB is second leaf blade, FthLB is forth leaf blade, ALF is Adult leaf, HP is Hypocotyl, TN is Tendril, JSM is juvenile stem, ASM is Adult stem, SAM is Shoot apical meristem. The color scale represents the level of expression (TPM value), from high (red) to low (blue). Gene expression data are downloaded from the Cucumber Multi-omics database.

bioRxiv preprint doi: https://doi.org/10.64898/2026.03.30.715073; this version posted April 1, 2026. The copyright holder for this preprint (which was not certified by peer review) is the author/funder, who has granted bioRxiv a license to display the preprint in perpetuity. It is made available under a CC-BY 4.0 International license.

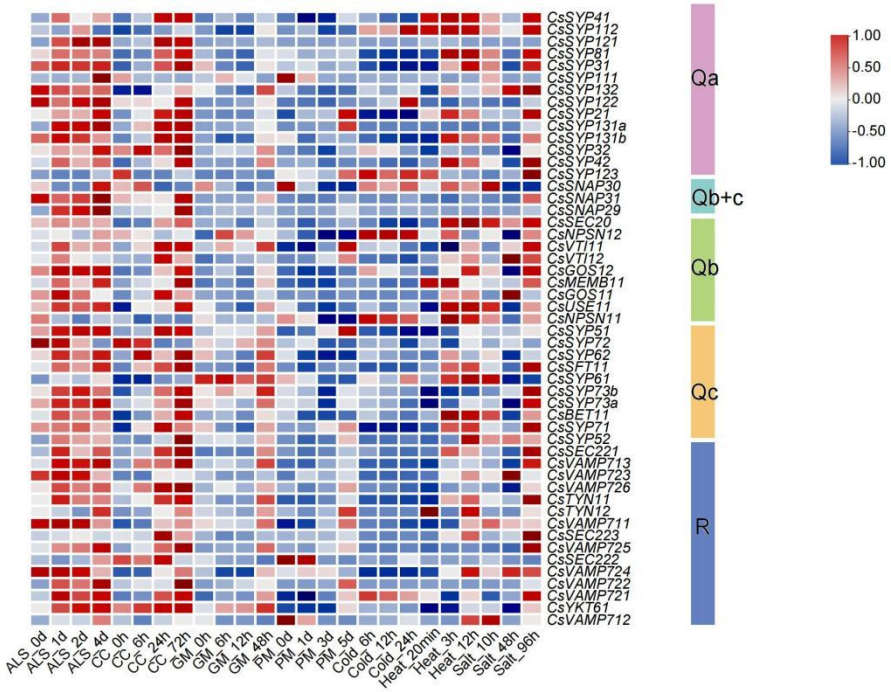

Fig. 7 The relative transcript levels of *CsSNARE* genes in Cucumber under different biological and abiotic stresses. ALS is angular leaf spot, CC is *Cladosporium cucumerium*, GM is Gray mold, PM is Powdery mildew. The color scale represents the level of expression (TPM value), from high (red) to low (blue). Gene expression data are downloaded from the Cucumber Multi-omics database.

bioRxiv preprint doi: https://doi.org/10.64898/2026.03.30.715073; this version posted April 1, 2026. The copyright holder for this preprint (which was not certified by peer review) is the author/funder, who has granted bioRxiv a license to display the preprint in perpetuity. It is made available under a CC-BY 4.0 International license.

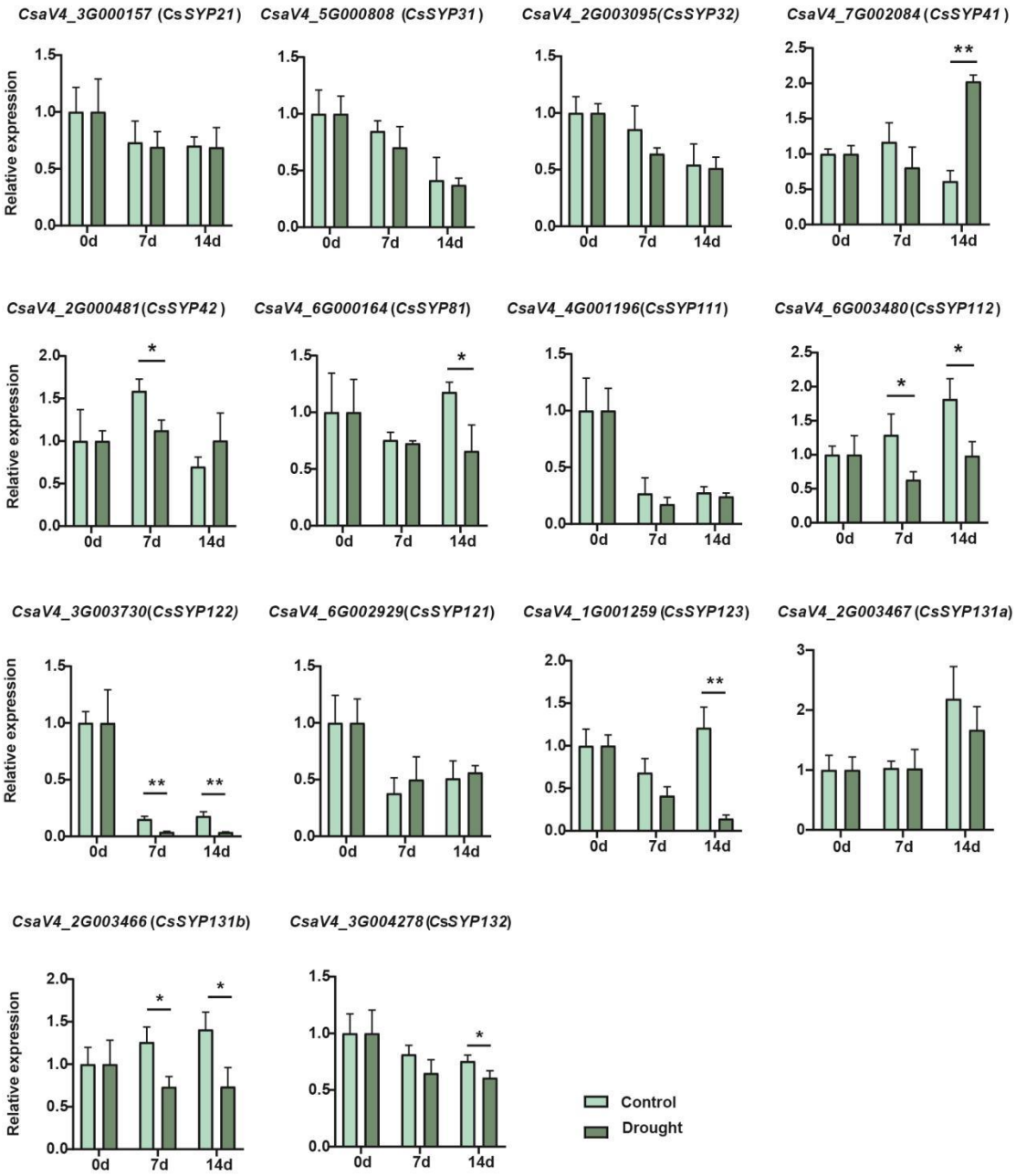

Fig. 8 Expression profiles of *Qa-CsSNARE* genes up-regulated or downregulated in Cucumber under drought stress. The qRT-PCR analyses were used to access transcript levels of *Qa-CsSNARE* genes with or without seven and fourteen days of drought treatment. Each bar represents the mean±SE normalized to *CsEF1α* (*CsaV4_5G001996*) and *CsCACS* (*CsaV4_3G004932*). All samples were run in three biological and three technical replicates. Light green columns represent "Control", and Dark green columns represent "Drought". Asterisk indicates that the gene expression under stress has a significant difference compared with the control (**P*<0.05, ***P*<0.01).

bioRxiv preprint doi: https://doi.org/10.64898/2026.03.30.715073; this version posted April 1, 2026. The copyright holder for this preprint (which was not certified by peer review) is the author/funder, who has granted bioRxiv a license to display the preprint in perpetuity. It is made available under a CC-BY 4.0 International license.

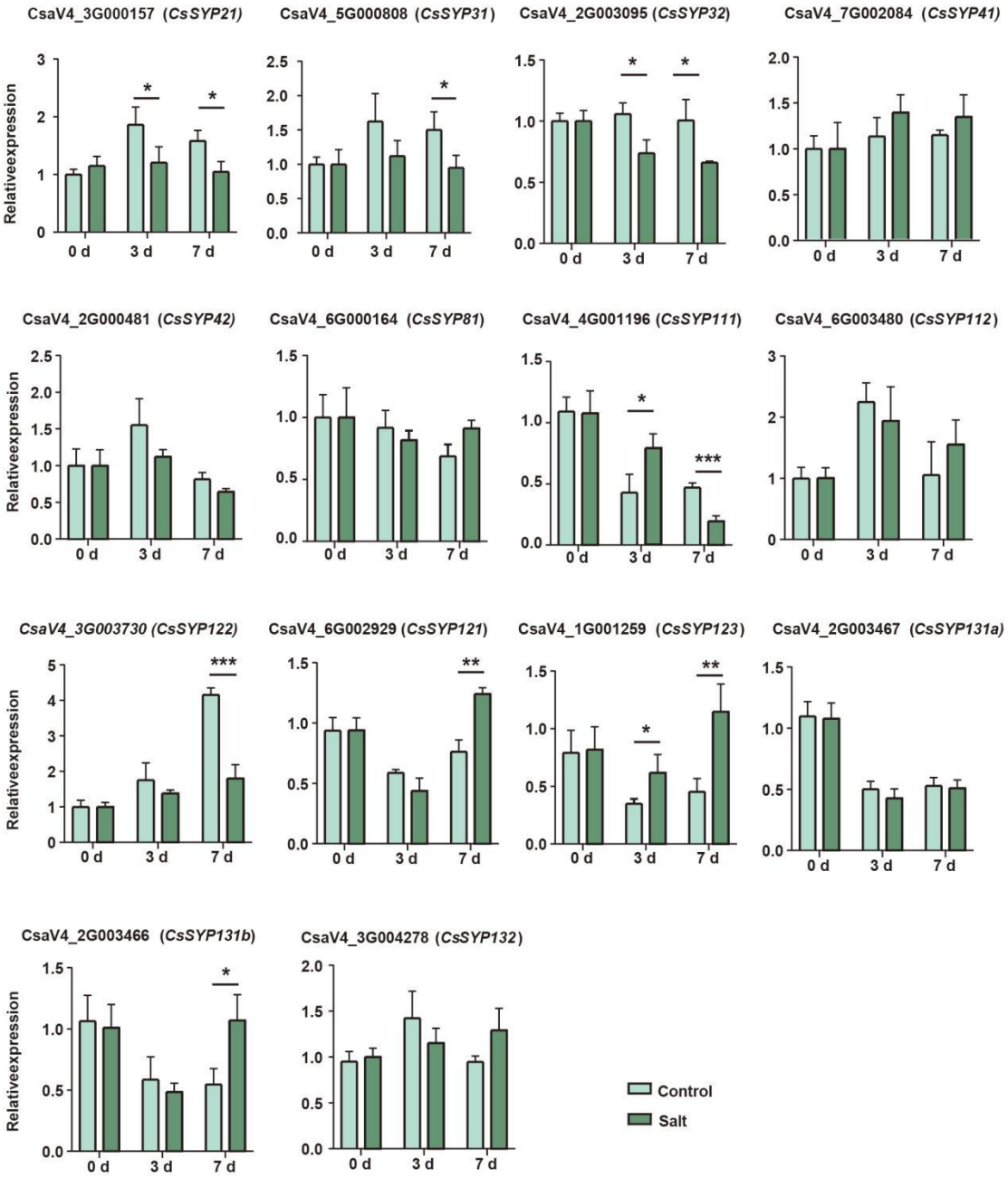

Fig. 9 Expression profiles of *Qa-CsSNARE* genes up-regulated or downregulated in wild-type cucumbers under salt stress. The qRT-PCR analyses were used to access transcript levels of *Qa-CsSNARE* genes with or without three and seven days of salt treatment. Each bar represents the mean±SE normalized to *CsEF1α* (*CsaV4_5G001996*) and *CsCACS* (*CsaV4_3G004932*). All samples were run in three biological and three technical replicates. Light green columns represent "Control", and Dark green columns represent "Salt". Asterisk indicates that the gene expression after stress has a significant difference compared with the control (**P*<0.05, ***P*<0.01, ****P*<0.001).

bioRxiv preprint doi: https://doi.org/10.64898/2026.03.30.715073; this version posted April 1, 2026. The copyright holder for this preprint (which was not certified by peer review) is the author/funder, who has granted bioRxiv a license to display the preprint in perpetuity. It is made available under a CC-BY 4.0 International license.

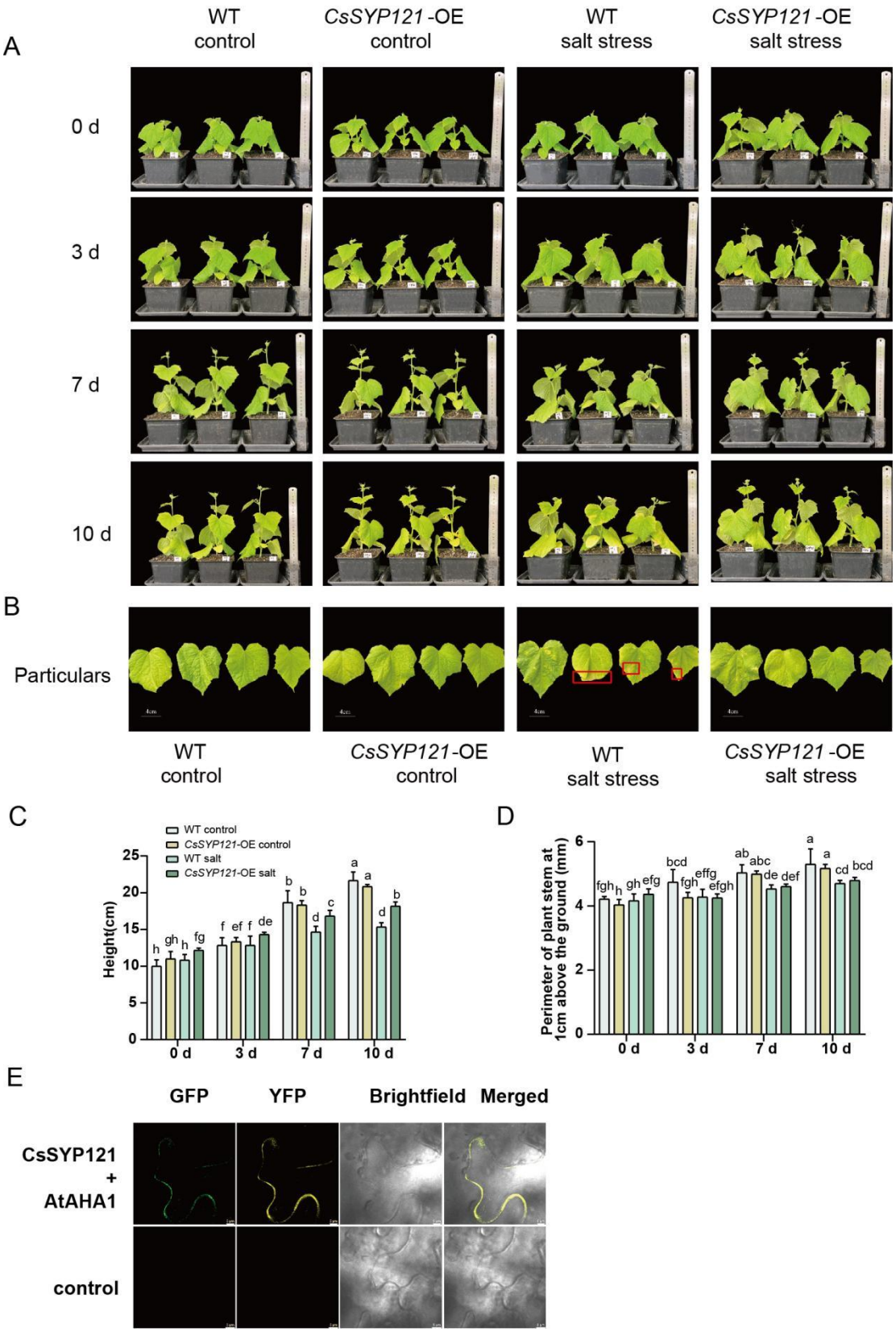

Fig. 10 Comparison of salt tolerance between *CsSYP121*-OE and wild-types cucumber plants. (A) The growth phenotypes of *CsSYP121*-OE and wild-types cucumber plants under salt stress of 0, 3 and 7

bioRxiv preprint doi: https://doi.org/10.64898/2026.03.30.715073; this version posted April 1, 2026. The copyright holder for this preprint (which was not certified by peer review) is the author/funder, who has granted bioRxiv a license to display the preprint in perpetuity. It is made available under a CC-BY 4.0 International license.

days. (B) The growth phenotypes and details of leaves of *CsSYP121*-OE and wild-types cucumber plants under salt stress for 10 days. The red boxes indicate leaves with significant phenotypic differences. (C) The plant heights of *CsSYP121*-OE and wild-types cucumber plants under salt stress of 0, 3 and 7 days. (D) Stem thickness of *CsSYP121*-OE and wild-types cucumber plants under salt stress of 0, 3, and 7 days. (E) Subcellular localization of CsSYP121. Images from left to right are GFP fluorescence (CsSYP121), YFP fluorescence (AtAHA1), bright field, and merged field of view, respectively. Brightfield shows the tobacco cells. Merged image represents the overlay of the three channels. Scale bar = 5 μm. Results are from three independent experiments (biological replicates, n=3). Data points represent the mean of each independent experiment, with error bars showing SEM. Different letters indicate significant differences (P<0.05).

bioRxiv preprint doi: https://doi.org/10.64898/2026.03.30.715073; this version posted April 1, 2026. The copyright holder for this preprint (which was not certified by peer review) is the author/funder, who has granted bioRxiv a license to display the preprint in perpetuity. It is made available under a CC-BY 4.0 International license.

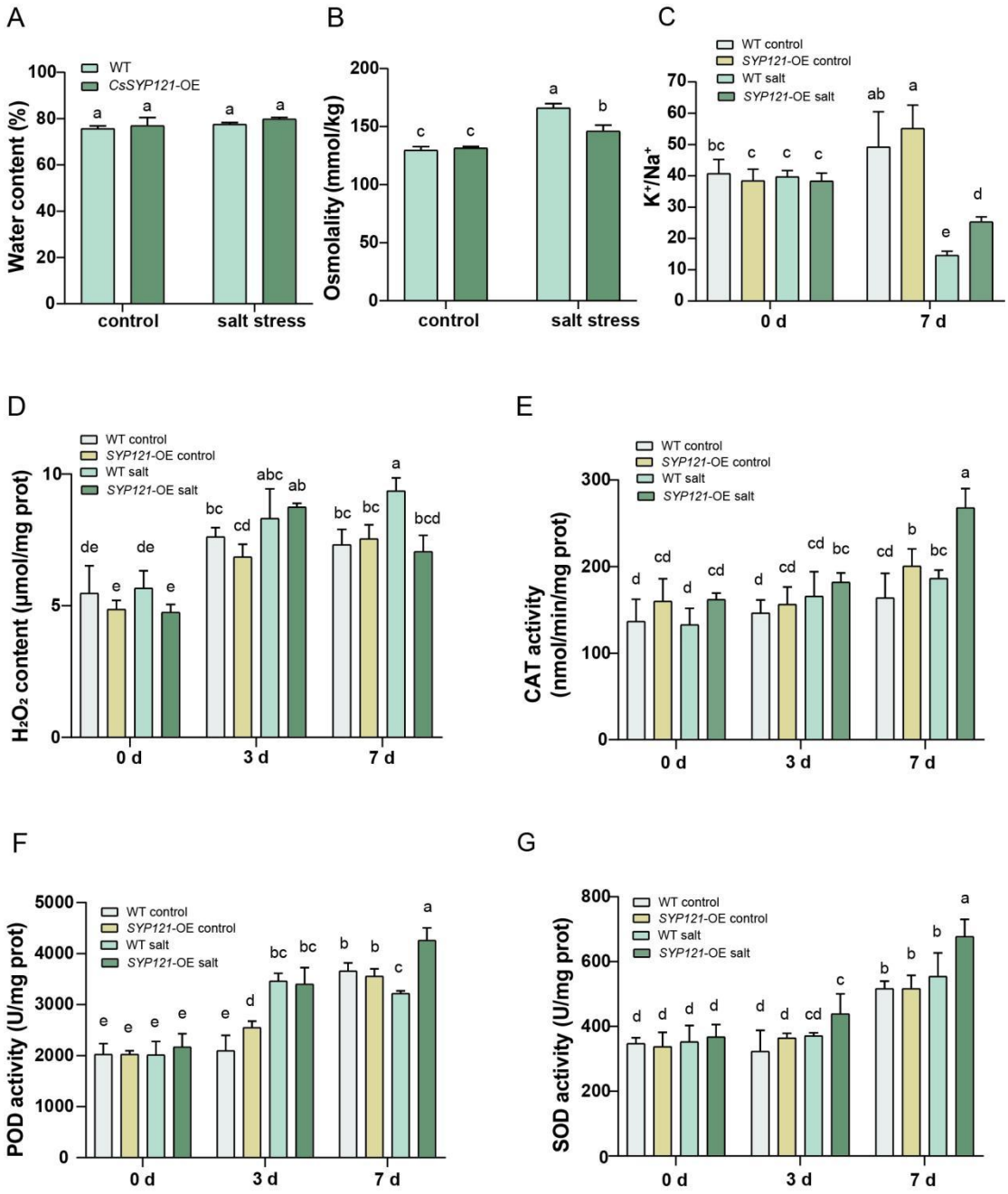

Fig. 11 The effects of salt stress on water content (A), osmotic pressure(B), K^+/Na^+ content ratio (C), H_2O_2 activity (D), CAT activity (E), POD activity (F), and SOD activity (G) of *SYP121*-OE and wild-type cucumbers. Results are from three independent experiments (biological replicates, n=3). Data points represent the mean of each independent experiment, with error bars showing SEM. Different letters indicate significant differences (P<0.05).